研究成果の刊行に関する一覧表

発表者氏名	論文タイトル名	発表誌名	巻号、頁	出版年
Kurachi S., Koizumi N., Sakurai F., Kawabata K., Sakurai H., Nakagawa S., Hayakawa T., Mizuguchi H.	Characterization of capsid-modified adenovirus vectors containing heterologous peptides in the fiber knob, protein IX, or hexon.	Gene Ther.	14, 266-274	2007
Kanayasu-Toyoda T., Suzuki T., Oshizawa T., Uchida E., Hayakawa T., Yamaguchi T.	Granulocyte colony-stimulating factor promotes the translocation of protein kinase Ci in neutrophilic differentiation cells.	Journal of Cell. Physiol.	211, 189-196	2007
Mizuguchi H., Funakoshi N., Hosono T., Sakurai F., Kawabata K., Yamaguchi T., Hayakawa T.	Rapid construction of small interfering RNA-expressing adenovirus vectors on the basis of direct cloning of short hairpin RNA-coding DNAs.	Hum. Gene Ther.	18, 74-80	2007
Koizumi N., Yamaguchi T., Kawabata K., Sakurai F., Sasaki T., Watanabe Y., Hayakawa T., Mizuguchi H.	Fiber- modified adenovirus vectors decrease liver toxicity through reduced interleukin 6 production.	J. Immunol.	178, 1767-17 73	2007
早川堯夫	Biotechnology （品質）に関するガイドラインの動向について	医薬品研究	38, 14-23	2007
Sakurai F., Akitomo K., Kawabata K., Hayakawa T., Mizuguchi H.	Downregulation of human CD46 by adenovirus serotype 35 vectors.	Gene Ther.	14, 912-919	2007
Kawai H., Suzuki T., Kobayashi T., Ishii-Watabe A., Sakurai H., Ohata H., Honda K., Momose K., Hayakawa T., Kawanishi T.	Caspase Cascade Proceeds Rapidly After Cytochrome c Release From Mitochondria in Tumor Necrosis Factor-alpha-Induced Cell Death.	J Pharmacol Sci.	103, 159-167	2007
早川堯夫	細胞基材の品質・安全性評価、バイオ医薬品の開発と品質・安全性確保 早川堯夫監修	バイオ医薬品の開発と品質・安全性確保 早川堯夫監修	51-67	2007
早川堯夫、福永悟史	感染性物質概論	バイオ医薬品の開発と品質・安全性確保 早	125-150	2007

		川堯夫監修		
早川堯夫	生物由来製品の指定	バイオ医薬品の開発と品質・安全性確保 早川堯夫監修	249-261	2007
早川堯夫	製品の特性解析・品質規格及び安定性	バイオ医薬品の開発と品質・安全性確保 早川堯夫監修	265-284	2007
川崎ナナ、早川堯夫	糖鎖構造解析	バイオ医薬品の開発と品質・安全性確保 早川堯夫監修	308-329	2007
堤康央、石井明子、早川堯夫	機能性人工タンパク質	バイオ医薬品の開発と品質・安全性確保 早川堯夫監修	369-378	2007
早川堯夫	コンパラビリティ及び後続品の評価 概論	バイオ医薬品の開発と品質・安全性確保 早川堯夫監修	381-399	2007
永田龍二、早川堯夫	非臨床における安全性評価ガイドライン	バイオ医薬品の開発と品質・安全性確保 早川堯夫監修	403-422	2007
早川堯夫、安藤 剛	細胞・組織利用医薬品等の品質及び安全性の確保	バイオ医薬品の開発と品質・安全性確保 早川堯夫監修	445-478	2007
早川堯夫、前田大輔、水口裕之	遺伝子治療用医薬品の品質、安全性等の確保	バイオ医薬品の開発と品質・安全性確保 早川堯夫監修	551-562	2007
水口裕之、早川堯夫	アデノウイルスベクター	バイオ医薬品の開発と品質・安全性確保 早川堯夫監修	563-577	2007
石井明子、鈴木琢雄、川西 徹、山口照英、早川堯夫	植物を用いた医薬品の現状と品質・安全性の確保	バイオ医薬品の開発と品質・安全性確保 早川堯夫監修	702-718	2007
Xin H., Kanehira M., Mizuguchi H., Hayakawa T.,	Targeted-Delivery of CX3CL1 to Multiple Lung Tumors by Mesenchymal Stem Cells.	Stem Cells	25, 1618-1626	2007

Kikuchi T., Nukiwa T., Saijo Y.				
Kawabata K., Tashiro K., Sakurai F., Osada N., Kusuda J., Hayakawa T., Yamanishi K., Mizuguchi H.	Positive and negative regulation of adenovirus infection by CAR-like soluble protein, CLSP.	Gene Ther.	14, 1199-1207	2007
早川堯夫	品質に関するトピックの動向（Quality Strategy Discussion）	医薬品研究	14, 1199-1207	2007
早川堯夫	バイオロジクス開発に関する規制と今後の動向	PHARMASTAGE	7, 1-4	2007
新見 伸吾，原島瑞，日向昌司，山口照英，早川堯夫	癌に対する抗血管新生療法の現状と展望 その1	医薬品研究	39, 1-37	2008
Moriuchi A., Yamasaki H., Shimamura M., Kita A., Kuwahara H., Fujishima K., Satoh T., Fukushima K., Fukushima T., Hayakawa T., Mizuguchi H., Nagayama Y., Abiru N., Kawasaki E., Eguchi K.	Induction of human adiponectin gene transcription by telmisartan, angiotensin receptor blocker, independently on PPAR- gamma activation.	Biochem Biophys. Res. Commun.	1024-1030	2007
Murakami S., Sakurai F., Kawabata K., Okada N., Fujita T., Yamamoto A., Hayakawa T., Mizuguchi H.	Interaction of penton base Arg-Gly-Asp motifs with integrins is crucial for adenovirus serotype 35 vector transduction in human hematopoietic cells.	Gene Ther.	14, 1525-1533	2007
早川堯夫	想像力と創造力	Drug Delivery System	22, 617	2007
早川堯夫	バイオ医薬品等をめぐる最近の動向と話題	ヒューマンサイエンス	19, 32-37	2008
Kanayasu-Toyoda T, Ishii-Watabe A, Suzuki T, Oshizawa T, Yamaguchi T.	A new role of thrombopoietin enhancing ex vivo expansion of endothelial precursor cells derived from AC133-positive cells.	J Biol Chem	282, 33507-33514	2007
山口照英	ヒト細胞治療薬の品質と安全性確保について	Bio Clinica	22, 1087-1094	2007
山口照英、土屋利江	細胞組織利用医薬品・医療機器の安全性とその有用性評価	Yakugaku zasshi	127, 839-40	2007

山口照英、内田恵理子	日米 EU 医薬品規制調和国際会議遺伝子治療専門家グループの活動と遺伝子治療薬の規制における国際動向	Drug Delivery System	22-26	2007
Hashii N, Kawasaki N, Nakajima Y, Toyoda M, Katagiri Y, Itoh S, Harazono A, Umezawa A, Yamaguchi T.	Study on the quality control of cell therapy products. Determination of N-glycolylneuraminic acid incorporated into human cells by nano-flow liquid chromatography/Fourier transforma -tion ion cyclotron mass spectrometry.	J Chromatogr A	1160: 263-269.	2007
内田恵理子、石井(渡部)明子、山口照英	遺伝子治療薬及び細胞治療薬のウイルス安全性確保	臨床とウイルス	35: 278-290	2007
Uchida E, Kogi M, Oshizawa T, Furuta B, Satoh K, Iwata A, Murata M, Hikata M, Yamaguchi T.	Optimization of the virus concentration method using polyethyleneimine-conjugated magnetic beads and its application to the detection of human hepatitis A, B and C viruses.	J Virol Methods	143: 95-103.	2007

Gene Therapy (2007) 14, 266–274

www.nature.com/gt

SHORT COMMUNICATION

Characterization of capsid-modified adenovirus vectors containing heterologous peptides in the fiber knob, protein IX, or hexon

S Kurachi[1,2], N Koizumi[1], F Sakurai[1], K Kawabata[1], H Sakurai[1,2], S Nakagawa[2], T Hayakawa[3] and H Mizuguchi[1,2]

[1]*Laboratory of Gene Transfer and Regulation, National Institute of Biomedical Innovation, Osaka, Japan;* [2]*Graduate School of Pharmaceutical Sciences, Osaka University, Osaka, Japan and* [3]*Pharmaceuticals and Medical Devices Agency, Tokyo, Japan*

Adenovirus (Ad) vectors are widely used in gene therapy and in vitro/in vivo *gene transfer because of their high transduction efficiency. However, Ad vector application in the gene therapy field is limited by poor transduction into cells not expressing the primary receptor, coxsackievirus and adenovirus receptor. To overcome this problem, several types of capsid-modified Ad vectors have been developed. The HI loop or C-terminus of the fiber knob, the C-terminus of the protein IX (pIX) and the hypervariable region 5 of the hexon are promising candidate locations for displaying foreign peptide sequences. In the present study, we constructed Ad vectors in which each of the above region was modified by a simple* in vitro *ligation-based method, and examined the characterization of each Ad vector containing the FLAG tag (DYKDDDDK) or RGD (CDCRGDCFC) peptide. Enzyme-linked immunosorbent assay examining the surface expression of foreign peptides on the virus suggested that foreign peptides are exposed on virion surfaces in all types vectors and that the hexon was the most efficiently reacted, reflecting the copy number of the modification. However, in the case of the transduction efficiency of Ad vectors containing the RGD peptides, the modification of pIX and the hexon showed no effect. The modification of the HI loop of the fiber knob was the most efficient, followed by the modification of the C-terminus region of the fiber knob. These comparative analyses, together with a simple construction method for each modified Ad vector, could provide basic information for the generation of capsid-modified Ad vectors.*
Gene Therapy (2007) **14**, 266–274. doi:10.1038/sj.gt.3302859; published online 28 September 2006

Keywords: *adenovirus; capside; fiber; protein IX; hexon*

Introduction

Adenovirus (Ad) vectors based on Ad type 5 are widely used for gene transfer studies and clinical gene therapy trials, since they can achieve high transduction efficiency and transduce into both dividing and non-dividing cells.[1,2] However, one of the hurdles confronting Ad-mediated gene transfer is that Ad infection is dependent on the expression levels of the coxsackievirus and adenovirus receptor (CAR) in the target cells. Ad vectors cannot transfer genes of interest into cells lacking CAR expression (i.e. many advanced tumor cells, peripheral blood cells, hematopoietic stem cells, dendritic cells, etc).[3,4]

Genetic modification of the Ad capsid, such as its fiber, protein IX (pIX), or hexon, is an attractive strategy for altering the Ad tropism. Among these options, modification of the fiber proteins has been the most widely studied. Fiber proteins consist of three distinct domains: the tail, shaft and knob. Each domain has distinct functions in host cell infection. The trimeric subunits of the C-terminal knob domain are responsible for binding to the host's primary cellular receptor, CAR.[5,6] Incorporation of the RGD (Arg-Gly-Asp) peptide or a stretch of lysine residues (K7 [KKKKKKK] peptide), which target αv integrins or heparan sulfate proteoglycans on the cellular surface, respectively, into the HI loop or the C-terminal region of the fiber knob allows Ad tropism to be expanded (or changed) by binding the modified fiber protein with the cellular receptor.[7–10]

The C-terminal region of pIX is another candidate location for capsid modification.[11] pIX is a minor structural protein contained in the Ad virion which enhances the structural integrity of the particles by stabilizing hexon–hexon interaction.[12,13] It also plays roles in transcriptional activity and nuclear reorganization.[14] The attractive characteristics of ligand insertion into the pIX region is that the C-terminus of pIX tolerates the insertion of large ligands.[15–17] As Ad pIX resides at a deep and hidden position below the tops of the hexon capsomer, Ad vectors containing the ligand-pIX fusion protein, which incorporates an α-helical spacer to sufficiently lift the ligands and expose them at the surface of the capsid, were developed.[18] Enhanced transduction was reported by Ad vectors containing the RGD peptide in the C-terminus of pIX with an α-helical spacer.[18]

Correspondence: Dr H Mizuguchi, Laboratory of Gene Transfer and Regulation, National Institute of Biomedical Innovation, Asagi 7-6-8, Saito, Ibaraki, Osaka 567-0085, Japan.
E-mail: mizuguch@nibio.go.jp
Received 8 March 2006; revised 17 July 2006; accepted 17 July 2006; published online 28 September 2006

Hexons are the most abundant capsid proteins and comprise each geometrical face of the capsid. As hexons are mostly targeted by neutralizing antibodies,[19] hexon modification has been reported to escape from neutralizing antibodies as well as to modify the tropism.[20] The hypervariable region (HVR) 5 of hexon loop L1 is a candidate location for incorporating foreign peptides without affecting the normal function of Ad type 5 as a gene transfer vector (i.e. viral growth, virus formation, virion stability, CAR-mediated infectivity).[21,22] Vigne *et al.*[21] have reported that Ad vectors containing the RGD peptides (DCRGDCF) at HVR5 of the hexon can infect cells via cellular αv integrin, independently of the CAR. However, Wu *et al.*[22] have reported that the His tag sequence at HVR5 had no effect on the transduction efficiency of Ad vectors when the vectors were applied to cells expressing anti-His tag single-chain antibody (scFv).

One attractive point of pIX or hexon modification is that 240 or 720 molecules of foreign peptides per virion are displayed at pIX or the hexon, respectively, while only 36 molecules are displayed at the fiber (note that the fiber and hexon are composed of trimeric subunits). Therefore, pIX- or hexon-modified Ad vectors containing heterologous peptides might be more effective than fiber-modified Ad vectors.

In the present study, we first developed a simple method for generating pIX- or hexon-modified Ad vectors by using *in vitro* ligation-based plasmid construction. The functionalities of Ad vectors containing the FLAG tag or RGD peptide in the HI loop or C-terminus of the fiber knob, C-terminus of pIX, or the HVR 5 region of the hexon were systemically compared. These comparative analyses could provide basic information for generation of capsid-modified Ad vectors.

First, we constructed newer vector plasmids pAdHM56 and -62, which we used for the generation of pIX- or hexon-modified Ad vectors, respectively. These contain a unique *Xba*I site in the coding regions of the C-terminal of pIX or HVR5 of the hexon, respectively (Figure 1), where only a minimal *Xba*I recognition sequence (TCTAGA) was introduced. pAdHM56 and -62 also contain unique I-*Ceu*I/*Swa*I/PI-*Sce*I sites in the E1 deletion region; hence, a transgene expression cassette can be cloned into the E1 deletion region by simple *in vitro* ligation, as previously described.[23,24] The shuttle plasmid pHM15-75A was constructed by introducing oligonucleotide 1/2, −3/4, −5/6, −7/8 (Table 1) into a derivative plasmid of pHM15.[25] pHM15-75A contains *Xba*I, *Avr*II, *Nhe*I and *Spe*I sites at both ends of a multicloning site and the coding sequence of a 75 Å α-helical spacer, as described by Vellinga *et al.*,[18] in the same multicloning site (Figure 1a). Detailed information about the constructions of the vector and shuttle plasmids is available from the authors upon request.

We previously developed a simple method for generating fiber-modified Ad vectors.[9,10] In that method, unique restriction enzyme sites (*Csp*45I and/or *Cla*I site) were introduced into the HI loop or C-terminal coding region of the fiber knob of the Ad vector plasmid, and the foreign DNA coding peptide of interest could easily be cloned into their regions by simple *in vitro* ligation.

In the present study, we expanded upon this system, so that heterologous peptide sequences could be inserted at the C-terminus region of pIX and the HVR5 region of the hexon. Figure 1 shows a representative example for generating Ad-RGD(pIX/75)-L2 and Ad-RGD(hexon)-L2, luciferase-expressing Ad vectors containing the RGD peptides in the C-terminus of the pIX via a 75 Å α-helical spacer and in the HVR5 region of the hexon, respectively. By using pHM15-75A, the peptide of interest coding sequence together with the 75 Å α-helical spacer coding sequence could easily be introduced into the C-terminal coding region of pIX of pAdHM56. As *Xba*I, *Avr*II, *Nhe*I and *Spe*I produce compatible cohesive ends, *Avr*II, *Nhe*I and *Spe*I sites as well as the *Xba*I site can be used for cloning into the *Xba*I site. Oligonucleotides corresponding to the peptide of interest can also be directly introduced into the *Xba*I site of pAdHM56. For the generation of pAdHM56-RGD75-L2, *Xba*I-digested pAdHM56-L2, in which a luciferase expression cassette was introduced into the E1 deletion region of pAdHM56 using I-*Ceu*I and PI-*Sce*I sites,[23,24] was ligated with *Avr*II-digested pHM15-75A-RGD, which was constructed by the introduction of oligonucleotides 9/10 corresponding to a GS linker plus the RGD-4C (CDCRGDCFC) peptide into the *Csp*45I/*Asc*I sites of pHM15-75A (Figure 1a). pAdHM62-RGD-L2, a vector plasmid for the hexon-modified Ad vector containing the RGD peptide, was constructed by the ligation of *Xba*I-digested pAdHM62-L2 with oligonucleotides 11/12, which contain a binding site with an *Xba*I-digested fragment and correspond to the RGD-4C peptide (Figure 1b). Oligonucleotides were designed so that the positive recombinant plasmid lacked an *Xba*I site for convenience of selection. Sequencing of all inserted oligonucleotides in each plasmid verified that the clones contained the appropriate sequences.

pAdHM56-FLAG-L2, pAdHM56-FLAG75-L2, pAdHM56-His-L2, pAdHM56-His75-L2, pAdHM56-RGD-L2 and pAdHM62-FLAG-L2 were similarly constructed as shown in Figure 1 by using *Xba*I-digested pAdHM56-L2 or pAdHM62-L2 with oligonucleotides 11–20. Ad vectors were generated by the transfection of *Pac*I-digested linearized vector plasmids described above into 293 cells and were prepared as described previously.[23,24] The conventional Ad vector (Ad-L2) and fiber-modified Ad vectors (Ad-RGD(HI)-L2 and Ad-RGD(C)-L2), had been previously constructed.[9,10] Determination of virus particle titers (VP) and infectious titer was accomplished spectrophotometrically by the method of Maizel *et al.*[26] and by using an Adeno-X Rapid Titer Kit (Clontech, Palo Alto, CA, USA), respectively. The infectious titer-to-particle ratio was 1:10 for Ad-L2, 1:17 for Ad-RGD(HI)-L2, 1:28 for Ad-RGD(C)-L2, 1:9 for Ad-RGD(pIX)-L2, 1:23 for Ad-RGD(pIX/75)-L2, 1:44 for Ad-RGD(hexon)-L2. All capsid-modified Ad vectors except Ad-RGD(hexon)-L2 were readily propagated, with similar particle titers to those of the conventional Ad vector, Ad-L2. The growth rate of Ad-RGD(hexon)-L2 was similar to that of Ad-L2, but the yield was approximately 10 times lower. Ad vectors and vector plasmids used in the present study are summarized in Table 2. All capsid-modified Ad vectors contain CAR and integrin binding motifs in the fiber and the penton base.

We then examined whether foreign peptides are displayed in the HI loop of the fiber knob, the C-terminus of the fiber knob, the C-terminus of pIX or the HVR5 region of the hexon (Figure 2). To do this, we generated capsid-modified Ad vectors containing the

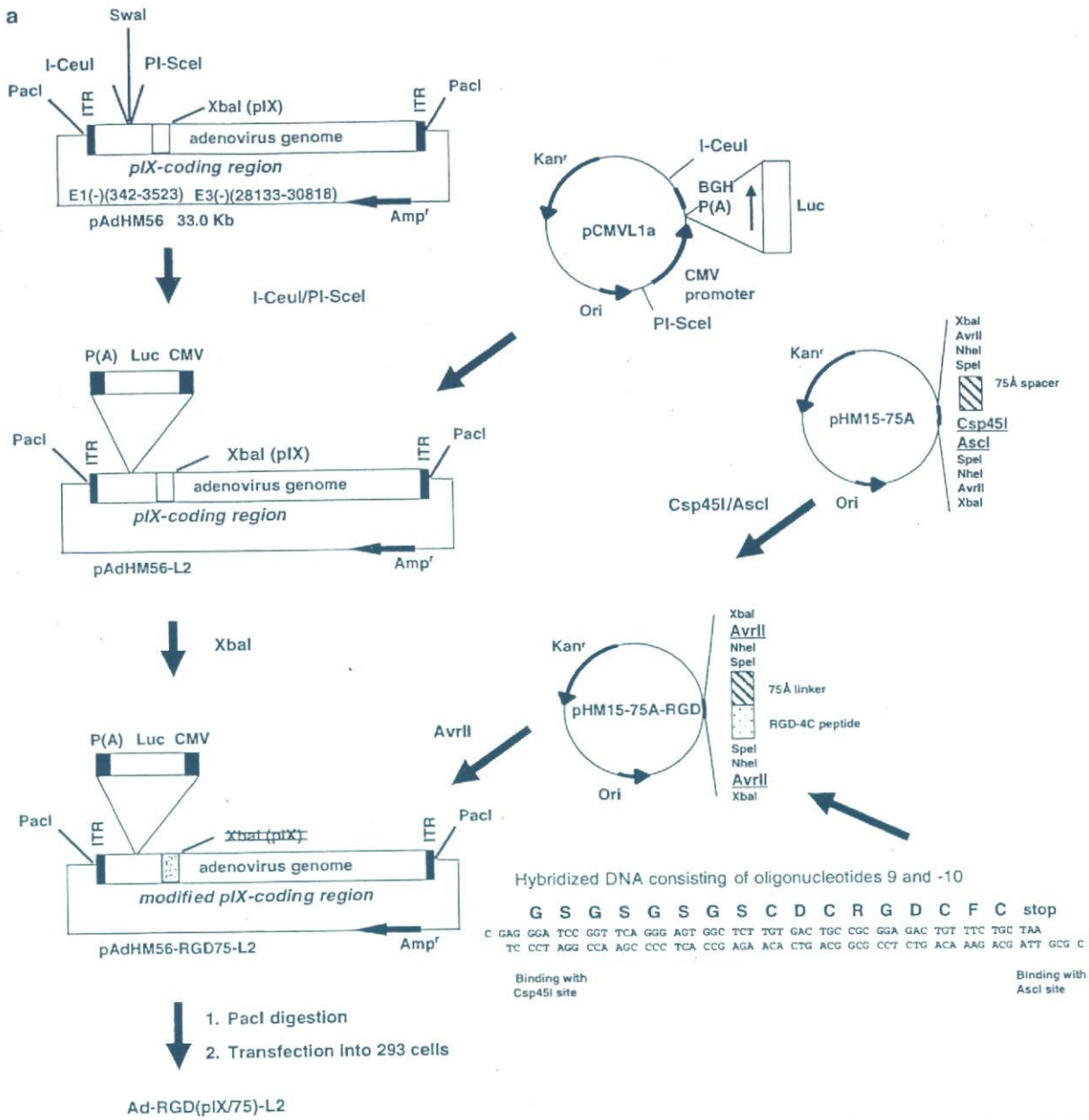

Figure 1 The construction strategy for pIX- or hexon-modified Ad vectors containing foreign peptides. (a) Construction of pIX-modified Ad vector. pAdHM56 was digested by I-*Ceu*I/PI-*Sce*I and ligated with I-*Ceu*I/PI-*Sce*I-digested pCMVL1a, which contains a CMV promoter-driven luciferase expression cassette, resulting in pAdHM56-L2. The shuttle plasmid pHM15-75A-RGD, which cloned oligonucleotides corresponding to the GS linker plus the RGD-4C peptide into pHM15-75A, was digested with *Avr*II and ligated with *Xba*I-digested pAdHM56-L2, resulting in pAdHM56-RGD75-L2. When *Avr*II, *Nhe*I or *Spe*I sites of the shuttle plasmid are used for cloning into the *Xba*I site of the vector plasmid, the positive recombinant plasmid lacks an *Xba*I site. Therefore, generation of the self-ligated plasmid is reduced by the digestion of the ligation sample with *Xba*I. A luciferase-expressing Ad vector containing the RGD peptide in the C-terminal of pIX with a 75 Å α-helical spacer, Ad-RGD(pIX/75)-L2, was produced by transfection of the *Pac*I-digested pAdHM56-RGD75-L2 into 293 cells. (b) Construction of hexon-modified Ad vector. pAdHM62-L2 was constructed by the ligation of I-*Ceu*I/PI-*Sce*I-digested pAdHM62 and I-*Ceu*I/PI-*Sce*I-digested pCMVL1a. Then, pAdHM62-L2 was digested with *Xba*I and ligated with an oligonucleotide corresponding to the linker (GS) and the RGD-4C peptide that contains a binding site with an *Xba*I-digested fragment, resulting in pAdHM62-RGD-L2. The oligonucleotide was designed so that the positive recombinant plasmid lacks an *Xba*I site. Generation of the self-ligated plasmid was reduced by the digestion of the ligation sample by *Xba*I. A luciferase-expressing Ad vector containing the RGD peptide in the HVR5 region of the hexon, Ad-RGD(hexon)-L2, was produced by transfection of the *Pac*I-digested pAdHM62-RGD-L2 into 293 cells.

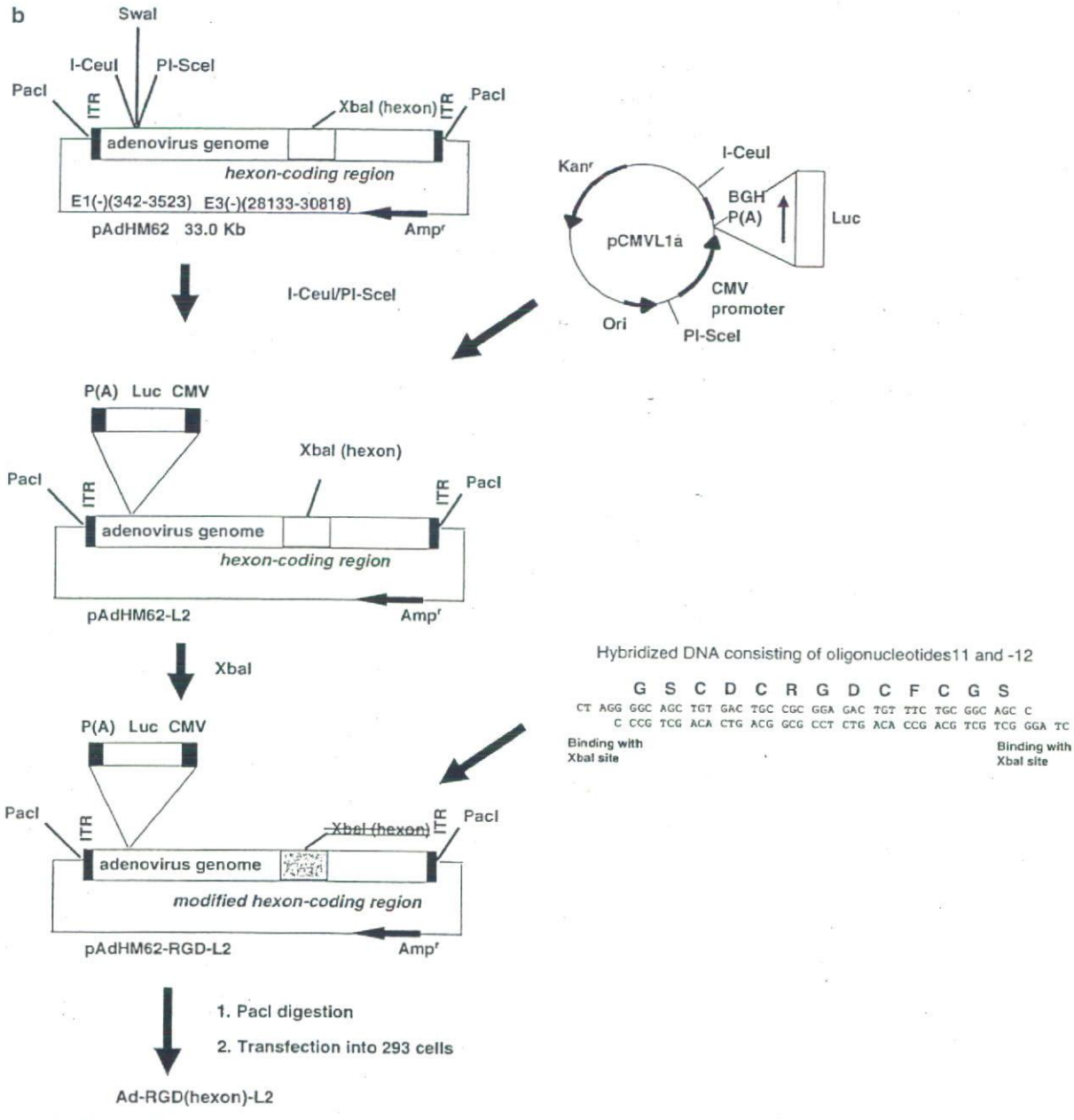

Figure 1 *Continued*

FLAG tag peptide in each region. Expression of the FLAG tag peptide in Ad-FLAG(HI)-L2, Ad-FLAG(C)-L2, Ad-FLAG(pIX)-L2 and Ad-FLAG(hexon)-L2 was examined by Western blotting. The total protein (1 μg) of each vector in 1 × sample buffer containing 4% β-mercaptoethanol was loaded on the SDS-PAGE gel after boiling 5 min, followed by electrotransfer to a PVDF (polyvinylidene difluoride) membrane. After blocking in Block Ace (Dainippon Pharmaceuticals, Osaka, Japan), the filters were incubated with ANTI-FLAG M2 monoclonal antibody (Sigma, Saint Louis, USA) (1:3000), followed by incubation in the presence of goat anti-mouse IgG HRP (Horseradish peroxidase)-linked antibody (Cell Signaling Technology Inc., MA, USA). The filters were developed by Chemi-Lumi One (Nacalai Tesque, Kyoto, Japan). The signals were read using a LAS-3000 machine (FUJIFILM, Tokyo, Japan). The FLAG tag peptide in the HI loop and the C-terminus of the fiber knob were about 60 kDa, similar size to a fiber protein. The molecular weight of pIX was 14.4 kDa and the FLAG tag peptide of Ad-FLAG(pIX)-L2 was about 14.4 kDa. The FLAG tag peptide detected in Ad-FLAG(hexon)-L2 was about 110 kDa, which is similar to the molecular weight of the hexon. Although the copy number of pIX is higher

Table 1 Oligonucleotides used in the present study

	Oligonucleotide	*Sequence of oligonucleotide (5′-3′)*
1	For 5′ region of 75 Å α-helical spacer (sense)	CTAGTTACAAGCTGGCCGACGAGGAGACGCGGGCACGGCTG TCCAAGGAGCTGCAGGCGGCGCAGGCCCGGCTGGGCGCGG ACATGGAGGACGTGTGC
2	For 5′ region of 75 Å α-helical spacer (antisense)	GGCCGCACACGTCCTCCATGTCCGCGCCCAGCCGGGCCTGC GCCGCCTGCAGCTCCTTGGACAGCCGTGCCCGCGTCTCCTC GTCGGCCAGCTTGTAA
3	For central region of 75 Å α-helical spacer (sense)	GGCCGCCTGGTGCAGTACCGCGGCGAGGTGCAGGCCATGCT CGGCCAGAGCACCGAGGAGCTGCGGGTGCGCCTCGCCTCCC ACCTGCGCAAGCTGCGTAAGCGGCTCG
4	For central region of 75 Å α-helical spacer (antisense)	TCGACGAGCCGCTTACGCAGCTTGCGCAGGTGGGAGGCGAG GCGCACCCGCAGCTCCTCGGTGCTCTGGCCGAGCATGGCCTG CACCTCGCCGCGGTACTGCACCAGGC
5	For 3′ region of 75 Å α-helical spacer (sense)	TCGAGATCCCAACCTATCTGAGCGAAGATGAACTGAAAGCC GCCGAAGCCGCCTTCAAACGCCACAACCCAACCGCGTTCGA AG
6	For 3′ region of 75 Å α-helical spacer (antisense)	GATCCTTCGAACGCGGTTGGGTTCTGGCGTTTGAAGGCGGCT TCGGCGGCTTTCAGTTCATCTTCGCTCAGATAGGTTGGGATC
7	For restriction enzyme sites from *Asc*I to *Xba*I at the downstream of 75 Å α-helical spacer of pHM15-75 A (sense)	AATTGGCGCGCCGCGGCCGCGTAAATGAATAGACTAGTGCTA GCCCTAGGTCTAGAGTGC
8	For restriction enzyme sites from *Asc*I to *Xba*I at the downstream of 75 Å α-helical spacer of pHM15-75 A (antisense)	TCTAGACCTAGGGCTAGCACTAGTCTATTCATTTACGCGGCCG CGGCGCGCC
9	For GS linker plus RGD-4C peptide into pHM15-75A (sense)	CGAGGGATCCGGTTCAGGGAGTGGCTCTTGTGACTGCCGCG GAGACTGTTTCTGCTAA
10	For GS linker plus RGD-4C peptide into pHM15-75A (antisense)	CGCGTTAGCAGAAACAGTCTCCGCGGCAGTCACAAGAGCCA CTCCCTGAACCGGATCCCT
11	For RGD-4C peptide into the C-terminus of pIX or HVR5 of hexon (sense)	CTAGGGGCAGCTGTGACTGCCGCGGAGACTGTTTCTGCGGCA GCC
12	For RGD-4C peptide into the C-terminus of pIX or HVR5 of hexon (antisense)	CTAGGGCTGCCGCAGAAACAGTCTCCGCGGCAGTCACAGCT GCCC
13	For FLAG tag sequence into the C-terminus of pIX or HVR5 of hexon (sense)	CTAGGGGCAGCGACTACAAGGACGATGATGACAAAGGCAG CC
14	For FLAG tag sequence into the C-terminus of pIX or HVR5 of hexon (antisense)	CTAGGGCTGCCTTTGTCATCATCGTCCTTGTAGTCGCTGCCC
15	For FLAG tag sequence into pHM15-75A (sense)	CGAGGGATCCGGTTCAGGGAGTGGCTCTGACTACAAGGACG ATGATGACAAATAA
16	For FLAG tag sequence into pHM15-75A (antisense)	CGCGTTATTTGTCATCATCGTCCTTGTAGTCAGAGCCACTCCC TGAACCGGATCCCT
17	For His tag sequence into the C-terminus of pIX (sense)	CTAGGGGCAGCCATCACCATCACCATCACGGCAGCC
18	For His tag sequence into the C-terminus of pIX (antisense)	CTAGGGCTGCCGTGATGGTGATGGTGATGGCTGCCC
19	For His tag sequence into pHM15-75A (sense)	CGAGGGATCCGGTTCAGGGAGTGGCTCTCATCACCATCACCA TCACTAA
20	For His tag sequence into pHM15-75A (antisense)	CGCGTTAGTGATGGTGATGGTGATGAGAGCCACTCCCTGAAC CGGATCCCT

than that of the fiber, the intensity of the band of Ad-FLAG(pIX)-L2 was weaker than that of Ad-FLAG(HI)-L2 and Ad-FLAG(C)-L2. This phenomenon is not due to impaired incorporation efficiency of the modified-pIX (at least the modified-pIX without the 75 Å α-helical spacer), because similar intensity of the pIX band was observed between Ad-FLAG(pIX)-L2 and Ad-L2 by Western blotting using anti-pIX antibody (kindly provided by Dr Keith N Leppard, Biological Sciences University of Warwick Coventry, UK)[27] (Figure 5b; will be described later). It remains unclear why the results of Figure 2 (anti-FLAG tag antibody) and Figure 5 (anti-pIX antibody) are different. The discrepancy might result from the property of each antibody. Anti-FLAG tag antibody is monoclonal, while anti-pIX antibody is polyclonal. These results suggested that the FLAG tag peptide was expressed as a fusion protein of the fiber, pIX or hexon.

Next, we examined by enzyme linked immunosorbent assay (ELISA) whether the FLAG tag peptide in each region was displayed on the virus surface (Figure 3). Purified viruses were incubated in carbonate-bicarbonate buffer (Sigma) and immobilized on a 96-well immunoplate (NALGE NUNC International, Tokyo, Japan) at 4°C. On the following day, wells were washed with phosphate buffered saline and blocked with Block Ace. Anti-FLAG tag monoclonal antibody (1:1000) diluted in Block Ace was bound to the immobilized virus and washed with phosphate-buffered saline containing 0.05% Tween20 (Polyxyethylene (20) Sorbitan Monolaurate; Wako Pure Chemical Industries Ltd, Osaka, Japan). Next, a secondary antibody (goat anti-mouse IgG HRP-linked antibody) diluted in Block Ace (1:1000) was bound to a mouse anti-FLAG tag antibody, and HRP was detected by TMB PEROXIDASE SUBSTRATE (MOSS Inc., Pasadena, ML, USA). Absorbance at 450–655 nm was measured by microplate reader. Ad-FLAG(HI)-L2, Ad-FLAG(C)-L2, Ad-FLAG(pIX)-L2 and Ad-FLAG(hexon)-L2 showed higher absorbance values than Ad-L2. Ad-FLAG(hexon)-L2 showed the highest absorbance values among all FLAG tag peptides displaying Ad vectors (Figure 3). The absorbance values were dependent on the copy number of the fusion protein on the

Table 2 Ad vectors used in the present study

Ad vectors	*Vector plasmids*	*Fiber*		*pIX*	*Hexon (HVR5)*
		HI loop	*C–terminus*		
Ad-L2	pAdHM4-L2	—	—	—	—
Ad-FLAG(HI)-L2	pAdHM41-FLAG(HI)-L2	DYKDDDDK	—	—	—
Ad-FLAG(C)-L2	pAdHM41-FLAG(C)-L2	—	$(GS)_4$DYKDDDDK	—	—
Ad-FLAG(pIX)-L2	pAdHM56-FLAG-L2	—	—	GSDYKDDDDKGS	—
Ad-FLAG(pIX/75)-L2	pAdHM56-FLAG75-L2	—	—	α-Helical linker plus $(GS)_4$DYKDDDDK	—
Ad-FLAG(hexon)-L2	pAdHM62-FLAG-L2	—	—	—	GSDYKDDDDKGS
Ad-His(pIX)-L2	pAdHM56-His-L2	—	—	GSHHHHHHGS	—
Ad-His(pIX/75)-L2	pAdHM56-His75-L2	—	—	α-Helical linker plus $(GS)_4$HHHHHH	—
Ad-RGD(HI)-L2	pAdHM15-RGD-L2	ACDCRGDCFCD	—	—	—
Ad-RGD(C)-L2	pAdHM41-RGD-L2	—	$(GS)_4$ACDCRGDCFCG	—	—
Ad-RGD(pIX)-L2	pAdHM56-RGD-L2	—	—	GSCDCRGDCFCGS	—
Ad-RGD(pIX/75)-L2	pAdHM56-RGD75-L2	—	—	α-helical linker plus $(GS)_4$CDCRGDCFC	—
Ad-RGD(hexon)-L2	pAdHM62-RGD-L2	—	—	—	GSCDCRGDCFCGS

Abbreviation: Ad, adenovirus.
Each modified Ad vector has additional amino-acids derived from unique restriction enzyme sites (*Csp*45I, *Cla*I or *Xba*I) in each region, but not be described here.

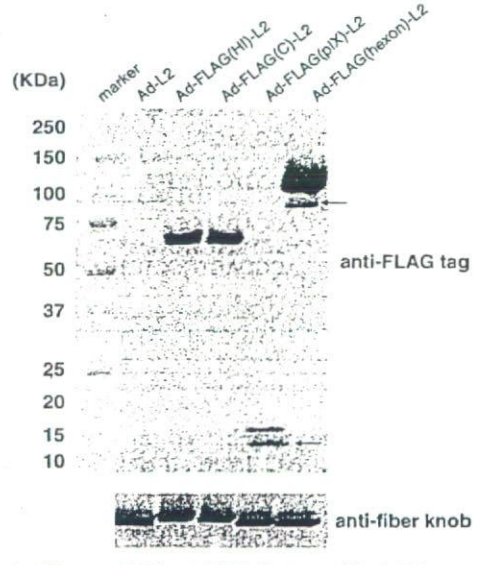

Figure 2 Western blotting of FLAG tag-modified Ad vectors. The total protein (1 μg) of each vector in 1 × sample buffer containing 4% β-mercaptoethanol was separated on a 4–20% SDS-PAGE gel, and the expression of the FLAG tag peptide was analyzed by Western blotting using mouse anti-FLAG tag monoclonal antibody. As a control, the membrane was also incubated with anti-fiber knob antibody (kindly provided by RD Gerard, University of Texas Southwestern Medical Center, Dallas, TX, USA). The band of the fiber of Ad-FLAG(HI)-L2 and Ad-FLAG(C)-L2 was higher than that of the other vectors, reflecting the insertion of the FLAG tag into the HI loop or C-terminus of the fiber knob. The extra bands marked with an arrow are proteolytic degradation products.

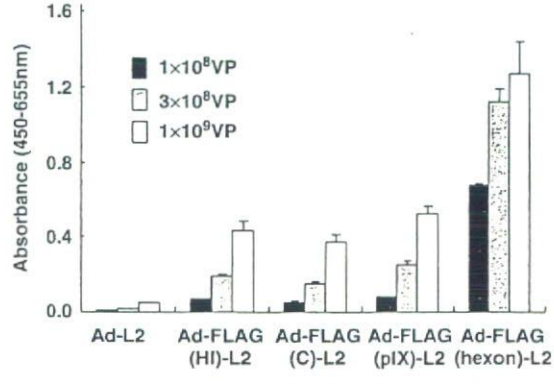

Figure 3 ELISA of FLAG tag-modified Ad vectors. Ad-L2, Ad-FLAG(HI)-L2, Ad-FLAG(C)-L2, Ad-FLAG(pIX)-L2 or Ad-FLAG(hexon)-L2 (10^9 VP/well, 3×10^8 VP/well, or 1×10^8 VP/well) were immobilized on a 96-well immunoplate. Mouse FLAG tag antibody was applied and then detected by anti-mouse IgG HRP-linked antibody. Absorbance at 450–655 nm was measured by microplate reader. The data are expressed as means ±s.d. ($n = 3$).

virus surface. Ad-FLAG(pIX)-L2, however, showed only slightly higher absorbance than Ad-FLAG(HI)-L2 and Ad-FLAG(C)-L2. ELISA is based on the ability of the anti-FLAG tag antibody to bind to the FLAG tag sequence on each Ad vector. The accessibility to the FLAG tag sequence at the C-terminus of pIX might be impaired, because pIX was buried between the hexon-tops. These results suggested that the fiber- (both the HI loop and C-terminus), pIX-, and the hexon-modified Ad vectors that were generated in this study did in fact display foreign ligands on the viral surface.

We and several groups have reported the feasibility of Ad vector application containing the RGD peptide in the HI loop or the C-terminus of the fiber knob, the C-terminus of pIX and the HVR5 region of the hexon.[9,10,18,21,28] However, there has been no report about which region is suitable for displaying the RGD peptide. To examine this, we constructed Ad vectors containing the RGD peptide in the fiber knob (HI loop or C-terminus), pIX (with or without 75 Å α-helical spacer),

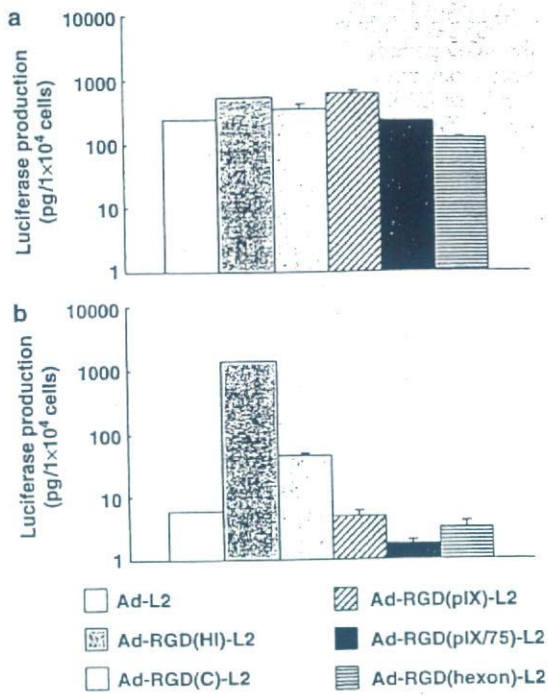

Figure 4 Transduction efficiency of RGD-modified Ad vectors. SK HEP-1 (a) and SF295 (b) cells were transduced with 3000 VP/cell of Ad-L2, Ad-RGD(HI)-L2, Ad-RGD(C)-L2, Ad-RGD(pIX)-L2, Ad-RGD(pIX/75A)-L2 or Ad-RGD(hexon)-L2 for 1.5 h, respectively. After culturing for 48 h, luciferase production was determined using a luciferase assay system (PicaGene LT2.0; Toyo Inki, Tokyo, Japan). The data are expressed as means ±s.d. ($n=3$).

and hexon and compared the luciferase production in SK HEP-1 and SF295 cells transduced with each vector (Figure 4). In the case of the pIX-modified Ad vector, the vector containing the 75 Å α-helical spacer between the C-terminus of pIX and the RGD peptide was also constructed as described previously,[18] together with the vector without the α-helical spacer. The RGD (CDCRGDCFC; RGD-4C) peptide binds to integrin αvβ3 and αvβ5 on the cellular surface.[29–31] SK HEP-1 cells were CAR-positive, while SF295 cells were CAR-negative. Both cells expressed αvβ3 and αvβ5 integrins (the expression of CAR and integrins in each cell was examined in our previous report by flow cytometry).[28] The luciferase enzymatic activity following transduction with Ad-RGD(HI)-L2, Ad-RGD(C)-L2, Ad-RGD(pIX)-L2, Ad-RGD(pIX/75)-L2 and Ad-RGD(hexon)-L2 was only about two to three times different from that with Ad-L2 in SK HEP-1 cells (Figure 4a). This would reflect that all vectors efficiently transduce via (at least) CAR. In contrast, in SF295 cells Ad-RGD(HI)-L2 and Ad-RGD(C)-L2 showed approximately 230- or 10-fold higher luciferase production, which mediated via an RGD-integrin-dependent pathway (our previous data and data not shown),[10,28] than Ad-L2 (Figure 4b). Luciferase production in SF295 cells transduced with Ad-RGD(pIX)-L2, Ad-RGD(pIX/75)-L2 and Ad-RGD(hexon)-L2 were not enhanced compared with Ad-L2. Lower luciferase production in SF295 cells transduced with Ad-RGD(hexon)-L2 was due to the about four times lower ratio of infectious titer-to-particle titer of Ad-RGD(hexon)-L2 in comparison with that of Ad-L2. These results suggested that the HI loop of the fiber knob is the most suitable region for capsid modification at least in the case of the insertion of the RGD peptide.

Vellinga *et al.*[18] reported that Ad vectors containing the RGD peptide at the C-terminus of pIX with a 75 Å α-helical spacer could transduce more efficiently into CAR-negative Eoma cells than vectors with a 30 or 45 Å α-helical spacer or no spacer. In the present study, we used a similar α-helical spacer sequence to that used by Vellinga *et al.*,[18] but no enhanced transduction was observed. The level of gene expression of Ad-RGD(pIX/75)-L2 was approximately three times lower in the SF295 cells than Ad-L2. We speculated that the lower transduction efficiency of Ad-RGD(pIX/75)-L2 might be due to the decreased incorporation efficiency of pIX-spacer-RGD into Ad-RGD(pIX/75)-L2. Therefore, we examined the incorporation of pIX into virus particles by Western blotting using the anti-pIX antibody (Figure 5a). The data obtained suggested that the incorporation efficiency of pIX-spacer-RGD into Ad-RGD(pIX/75)-L2 was greatly decreased, and only a faint band (marked with an asterisk) was observed, while that of pIX-RGD into Ad-RGD(pIX)-L2 was similar to that into Ad-L2, a control virus (Figure 5a). Therefore, a longer spacer might hamper incorporation efficiency. This would be the reason why Ad-RGD(pIX/75)-L2 did not show increased transduction efficiency. To examine this phenomenon in more detail, the incorporation of modified-pIX with the FLAG tag or His tag (HHHHHH) peptide into each virus was examined instead of the RGD peptide (Figure 5b). Modified-pIX without the spacer (Ad-FLAG(pIX)-L2 and Ad-His(pIX)-L2) was similarly incorporated into the wild-type virus (Ad-L2), while that with the spacer (Ad-FLAG(pIX/75)-L2 and Ad-His(pIX/75)-L2) was severely impaired. When the vectors were over-loaded on the SDS-PAGE gel, the band of the RGD-, FLAG tag- or His tag-modified pIX with a longer spacer was observed. Therefore, incorporation efficiency of modified-pIX was not completely impaired (Figure 5c). The pIX-spacer-His tag peptide was more efficiently incorporated into Ad-His(pIX/75)-L2 than the pIX-spacer-FLAG into Ad-FLAG(pIX/75)-L2, suggesting that the kind of peptide inserted might affect the incorporation efficiency when the longer spacer sequence is used. Vellinga *et al.*[18] reported the generation of pIX-modified Ad vector with a longer spacer by co-transfection of vector plasmid lacking pIX coding region and the plasmid expresses a series of modified pIX. The incorporation efficiency of pIX with a longer spacer into virion was lower than that of conventional-pIX, although their efficiency was higher than that in the present study. Subtle differences in the linker sequence between pIX and the longer spacer or between the longer spacer and the RGD peptide might have caused this difference in results. Their group recently reported new method for generation of pIX-modified Ad vectors.[32] They created a series of helper cell lines producing modified-pIX with and without longer spacers. The incorporation efficiency of pIX with a longer spacer into virion generated by the method was similar to that of unmodified-pIX. They also showed that the heat-stability of pIX-modified Ad vector with a longer spacer was worse than that of the

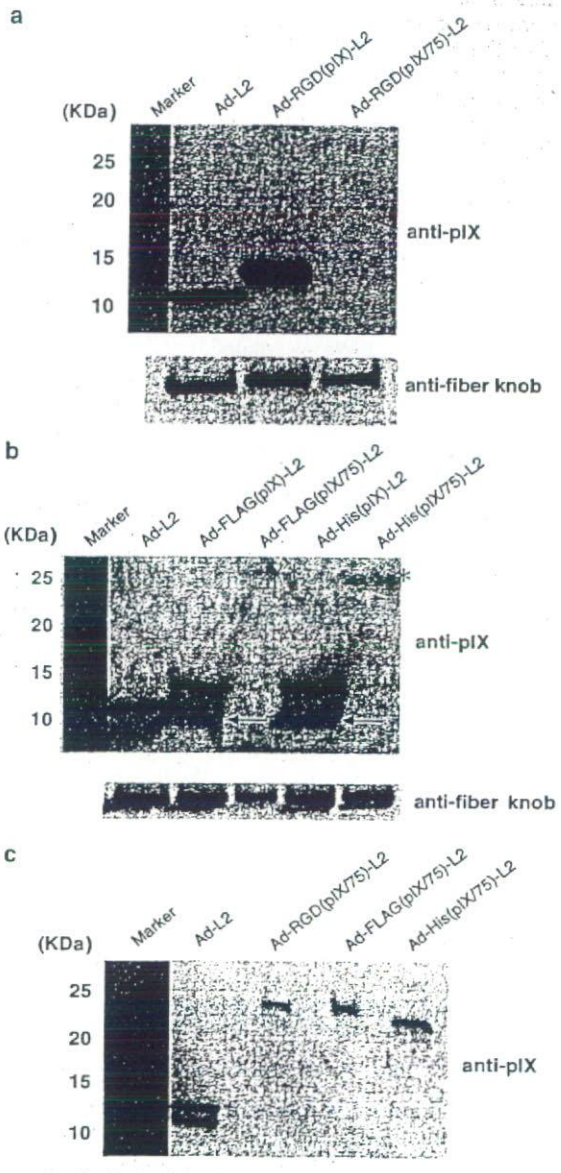

Figure 5 Analysis of the incorporation efficiency of modified-pIX. Incorporation efficiency of modified-pIX into the virus particles was determined by Western blotting. The total protein (a and b, 1 μg; c, 10 μg) of each vector in 1× sample buffer containing 4% β-mercaptoethanol was separated on a 4–20% SDS-PAGE gel, and pIX was detected by the anti-pIX antibody. As a control, the anti-fiber knob antibody was used. (a) pIX-modified Ad vector containing the RGD peptide with or without a 75 Å α-helical spacer. (b) pIX-modified Ad vector containing the FLAG tag or His tag peptide with or without a 75 Å α-helical spacer. Ad-FLAG(pIX/75)-L2, Ad-His(pIX)-L2 and Ad-His(pIX/75)-L2 containing the FLAG tag or His tag peptide in the C-terminus of the pIX with or without a 75 Å α-helical spacer were similarly generated, as shown in Figure 1a. (c) The pIX-modifed Ad vector containing the RGD, FLAG tag, or His tag peptide with a 75 Å α-helical spacer. The extra bands marked with an arrow are proteolytic degradation products. The asterisks indicate the band of the modified-pIX with a 75 Å α-helical spacer.

conventional Ad vector and pIX-modified Ad vector without longer spacer. For these reasons, care should be taken in the use of a longer spacer.

Vigne *et al*.[21] have reported that Ad vectors containing the RGD peptide (DCRGDCF) at the HVR5 region of the hexon can infect cells via cellular αv integrin independently of CAR, which was inconsistent with the present study. The precise mechanism for these differences remains unclear. Subtle differences in the inserted RGD peptide sequence (SRGSCDCRGDCFCGSPR including the restriction enzyme-coding sequence in our study and GSDCRGDCFGS in their study) or the difference in the cell types used might have caused the discrepancy in results.

After we submitted this manuscript, Campos and Barry[33] reported a similar study in which fiber-, pIX- and hexon-modification were compared. They generated metabolically biotinylated Ad vectors by the insertion of the biotin acceptor peptide (BAP) in each location to directly compare targeted transduction through the fiber, pIX and hexon using a variety of biotinylated ligands, such as antibodies and proteins, which had a higher affinity than the RGD peptide. They reported that the modification of the fiber was more efficient than that of pIX and hexon,[33] which is consistent with the present report. They discussed how high affinity ligands at pIX or hexon made it impossible for the virus to escape from the endosome, and enter the cytoplasm, and traffic to the nucleus because the interaction between ligands at pIX or hexon and the cellular receptor was very strong. In the present study, we chose the RGD peptide to change (or expand) the tropism of the Ad vector, which had a lower affinity than antibodies or proteins. The modification of pIX and hexon with the RGD peptide might also have affected intracellular trafficking.

One of the possible reasons why the HI loop of the fiber knob is efficient in the case of the RGD peptide is that peptides displayed in the fiber knob can easily access the target molecules (receptors) because fiber knobs are the outmost capsid proteins of Ad vectors (the HI loop of the fiber knob is more exposed than the C-terminus). Therefore, pIX-modified or hexon-modified Ad vectors without the fiber proteins might show efficient ligand-mediated transduction because the ligand can come close to the cellular surface receptor. In addition, fiber-less Ad vectors do not infect cells via CAR due to the lack of fiber proteins.[34,35] pIX-modified or hexon-modified Ad vectors without fiber proteins could be a platform vector for targeting, although the fiber-less Ad vector was weaker against physical burdens, such as heat-treatment and freeze-and-thaw, than the conventional Ad vector (our unpublished data).

In summary, we have developed a simple method based on *in vitro* ligation to construct Ad vectors containing heterologous peptides in the C-terminus of pIX or the HVR5 region of the hexon. These Ad vectors displayed foreign peptides on the viral surface in each region. In the case of the insertion of the RGD peptide, Ad vectors modified in the HI loop of the fiber knob proved the better choice. As the vector system shown here enables easy construction of capsid-modified Ad vectors displaying a peptide of interest, it has great potential for gene therapy and gene transfer experiments.

Acknowledgements

The author thanks Tomomi Sasaki for technical assistance. This work was supported by grants from the

Ministry of Health, Labor, and Welfare of Japan. NK is the recipient of a fellowship from the Japan Society for the Promotion of Science.

References

1 Kovesdi I, Brough DE, Bruder JT, Wickham TJ. Adenoviral vectors for gene transfer. *Curr Opin Biotechnol* 1997; 8: 583–589.
2 Benihoud K, Yeh P, Perricaudet M. Adenovirus vectors for gene delivery. *Curr Opin Biotechnol* 1999; 10: 440–447.
3 Wickham TJ. Targeting adenovirus. *Gene Therapy* 2000; 7: 110–114.
4 Mizuguchi H, Hayakawa T. Targeted adenovirus vectors. *Hum Gene Ther* 2004; 15: 1034–1044.
5 Bergelson JM, Cunningham JA, Droguett G, Kurt-Jones EA, Krithivas A, Hong JS *et al*. Isolation of a common receptor for Coxsackie B viruses and adenoviruses 2 and 5. *Science* 1997; 275: 1320–1323.
6 Tomko RP, Xu R, Philipson L. HCAR and MCAR: the human and mouse cellular receptors for subgroup C adenoviruses and group B coxsackieviruses. *Proc Natl Acad Sci USA* 1997; 94: 3352–3356.
7 Dmitriev I, Krasnykh V, Miller CR, Wang M, Kashentseva E, Mikheeva G *et al*. An adenovirus vector with genetically modified fibers demonstrates expanded tropism via utilization of a coxsackievirus and adenovirus receptor-independent cell entry mechanism. *J Virol* 1998; 72: 9706–9713.
8 Staba MJ, Wickham TJ, Kovesdi I, Hallahan DE. Modifications of the fiber in adenovirus vectors increase tropism for malignant glioma models. *Cancer Gene Ther* 2000; 7: 13–19.
9 Mizuguchi H, Koizumi N, Hosono T, Utoguchi N, Watanabe Y, Kay MA *et al*. A simplified system for constructing recombinant adenoviral vectors containing heterologous peptides in the HI loop of their fiber knob. *Gene Therapy* 2001; 8: 730–735.
10 Koizumi N, Mizuguchi H, Utoguchi N, Watanabe Y, Hayakawa T. Generation of fiber-modified adenovirus vectors containing heterologous peptides in both the HI loop and C terminus of the fiber knob. *J Gene Med* 2003; 5: 267–276.
11 Dmitriev IP, Kashentseva EA, Curiel DT. Engineering of adenovirus vectors containing heterologous peptide sequences in the C terminus of capsid protein IX. *J Virol* 2002; 76: 6893–6899.
12 Ghosh-Choudhury G, Haj-Ahmad Y, Graham FL. Protein IX, a minor component of the human adenovirus capsid, is essential for the packaging of full length genomes. *EMBO J* 1987; 6: 1733–1739.
13 Furcinitti PS, van Oostrum J, Burnett RM. Adenovirus polypeptide IX revealed as capsid cement by difference images from electron microscopy and crystallography. *EMBO J* 1989; 8: 3563–3570.
14 Rosa-Calatrava M, Grave L, Puvion-Dutilleul F, Chatton B, Kedinger C. Functional analysis of adenovirus protein IX identifies domains involved in capsid stability, transcriptional activity, and nuclear reorganization. *J Virol* 2001; 75: 7131–7141.
15 Le LP, Everts M, Dmitriev IP, Davydova JG, Yamamoto M, Curiel DT. Fluorescently labeled adenovirus with pIX-EGFP for vector detection. *Mol Imag* 2004; 3: 105–116.
16 Meulenbroek RA, Sargent KL, Lunde J, Jasmin BJ, Parks RJ. Use of adenovirus protein IX (pIX) to display large polypeptides on the virion–generation of fluorescent virus through the incorporation of pIX-GFP. *Mol Ther* 2004; 9: 617–624.
17 Li J, Le L, Sibley DA, Mathis JM, Curiel DT. Genetic incorporation of HSV-1 thymidine kinase into the adenovirus protein IX for functional display on the virion. *Virology* 2005; 338: 247–258.
18 Vellinga J, Rabelink MJ, Cramer SJ, van den Wollenberg DJ, Van der Meulen H, Leppard KN *et al*. Spacers increase the accessibility of peptide ligands linked to the carboxyl terminus of adenovirus minor capsid protein IX. *J Virol* 2004; 78: 3470–3479.
19 Sumida SM, Truitt DM, Lemckert AA, Vogels R, Custers JH, Addo MM *et al*. Neutralizing antibodies to adenovirus serotype 5 vaccine vectors are directed primarily against the adenovirus hexon protein. *J Immunol* 2005; 174: 7179–7185.
20 Roberts DM, Nanda A, Havenga MJ, Abbink P, Lynch DM, Ewald BA *et al*. Hexon-chimaeric adenovirus serotype 5 vectors circumvent pre-existing anti-vector immunity. *Nature* 2006; 441: 239–243.
21 Vigne E, Mahfouz I, Dedieu JF, Brie A, Perricaudet M, Yeh P. RGD inclusion in the hexon monomer provides adenovirus type 5-based vectors with a fiber knob-independent pathway for infection. *J Virol* 1999; 73: 5156–5161.
22 Wu H, Han T, Belousova N, Krasnykh V, Kashentseva E, Dmitriev I *et al*. Identification of sites in adenovirus hexon for foreign peptide incorporation. *J Virol* 2005; 79: 3382–3390.
23 Mizuguchi H, Kay MA. A simple method for constructing E1- and E1/E4-deleted recombinant adenoviral vectors. *Hum Gene Ther* 1999; 10: 2013–2017.
24 Mizuguchi H, Kay MA. Efficient construction of a recombinant adenovirus vector by an improved in vitro ligation method. *Hum Gene Ther* 1998; 9: 2577–2583.
25 Mizuguchi H, Xu ZL, Sakurai F, Mayumi T, Hayakawa T. Tight positive regulation of transgene expression by a single adenovirus vector containing the rtTA and tTS expression cassettes in separate genome regions. *Hum Gene Ther* 2003; 14: 1265–1277.
26 Maizel Jr JV, White DO, Scharff MD. The polypeptides of adenovirus. I. Evidence for multiple protein components in the virion and a comparison of types 2, 7A, and 12. *Virology* 1968; 36: 115–125.
27 Caravokyri C, Leppard KN. Constitutive episomal expression of polypeptide IX (pIX) in a 293-based cell line complements the deficiency of pIX mutant adenovirus type 5. *J Virol* 1995; 69: 6627–6633.
28 Koizumi N, Mizuguchi H, Hosono T, Ishii-Watabe A, Uchida E, Utoguchi N *et al*. Efficient gene transfer by fiber-mutant adenoviral vectors containing RGD peptide. *Biochim Biophys Acta* 2001; 1568: 13–20.
29 Koivunen E, Wang B, Ruoslahti E. Phage libraries displaying cyclic peptides with different ring sizes: ligand specificities of the RGD-directed integrins. *Biotechnology (New York)* 1995; 13: 265–270.
30 Pasqualini R, Koivunen E, Ruoslahti E. Alpha v integrins as receptors for tumor targeting by circulating ligands. *Nat Biotechnol* 1997; 15: 542–546.
31 Arap W, Pasqualini R, Ruoslahti E. Cancer treatment by targeted drug delivery to tumor vasculature in a mouse model. *Science* 1998; 279: 377–380.
32 Vellinga J, Uil TG, de Vrij J, Rabelink MJ, Lindholm L, Hoeben RC. A system for efficient generation of adenovirus protein IX-producing helper cell lines. *J Gene Med* 2006; 8: 147–154.
33 Campos SK, Barry MA. Comparison of adenovirus fiber, protein IX, and hexon capsomeres as scaffolds for vector purification and cell targeting. *Virology* 2006; 349: 453–462.
34 Legrand V, Spehner D, Schlesinger Y, Settelen N, Pavirani A, Mehtali M. Fiberless recombinant adenoviruses: virus maturation and infectivity in the absence of fiber. *J Virol* 1999; 73: 907–919.
35 Von Seggern DJ, Chiu CY, Fleck SK, Stewart PL, Nemerow GR. A helper-independent adenovirus vector with E1, E3, and fiber deleted: structure and infectivity of fiberless particles. *J Virol* 1999; 73: 1601–1608.

Journal of Cellular Physiology

Granulocyte Colony-Stimulating Factor Promotes the Translocation of Protein Kinase Cι in Neutrophilic Differentiation Cells

TOSHIE KANAYASU-TOYODA,[1] TAKAYOSHI SUZUKI,[1] TADASHI OSHIZAWA,[1] ERIKO UCHIDA,[2] TAKAO HAYAKAWA,[2] AND TERUHIDE YAMAGUCHI[1]*

[1]*Division of Cellular and Gene Therapy Products, National Institute of Health Sciences, Tokyo, Japan*

[2]*National Institute of Health Sciences, Tokyo, Japan*

Previously, we suggested that the phosphatidylinositol 3-kinase (PI3K)-p70 S6 kinase (p70 S6K) pathway plays an important role in granulocyte colony-stimulating factor (G-CSF)-dependent enhancement of the neutrophilic differentiation and proliferation of HL-60 cells. While atypical protein kinase C (PKC) has been reported to be a regulator of p70 S6K, abundant expression of PKCι was observed in myeloid and lymphoid cells. Therefore, we analyzed the participation of PKCι in G-CSF-dependent proliferation. The maximum stimulation of PKCι was observed from 15 to 30 min after the addition of G-CSF. From 5 to 15 min into this lag time, PKCι was found to translocate from the nucleus to the membrane. At 30 min it re-translocated to the cytosol. This dynamic translocation of PKCι was also observed in G-CSF-stimulated myeloperoxidase-positive cells differentiated from cord blood cells. Small interfering RNA for PKCι inhibited G-CSF-induced proliferation and the promotion of neutrophilic differentiation of HL-60 cells. These data indicate that the G-CSF-induced dynamic translocation and activation processes of PKCι are important to neutrophilic proliferation.

J. Cell. Physiol. 211: 189–196, 2007.

Hematopoietic cell differentiation is regulated by a complex network of growth and differentiation factors (Tenen et al., 1997; Ward et al., 2000). Granulocyte colony-stimulating factor (G-CSF) and its receptors are pivotal to the differentiation of myeloid precursors into mature granulocytes. In previous studies (Kanayasu-Toyoda et al., 2002) on the neutrophilic differentiation of HL-60 cells treated with either dimethyl sulfoxide (DMSO) or retinoic acid (RA), heterogeneous transferrin receptor (Trf-R) populations—transferrin receptor-positive ($Trf\text{-}R^+$) cells and transferrin receptor-negative ($Trf\text{-}R^-$) cells—appeared 2 days after the addition of DMSO or RA. The $Trf\text{-}R^+$ cells were proliferative-type cells that had higher enzyme activity of phosphatidylinositol 3-kinase (PI3K) and protein 70 S6 kinase (p70 S6K), whereas the $Trf\text{-}R^-$ cells were differentiation-type cells of which Tyr705 in STAT3 was much more phosphorylated by G-CSF. Inhibition of either PI3K by wortmannin or p70 S6K by rapamycin was found to eliminate the difference in differentiation and proliferation abilities between $Trf\text{-}R^+$ and $Trf\text{-}R^-$ cells in the presence of G-CSF (Kanayasu-Toyoda et al., 2002). From these results, we concluded that proteins PI3K and p70 S6K play important roles in the growth of HL-60 cells and negatively regulate neutrophilic differentiation. On the other hand, the maximum kinase activity of PI3K was observed at 5 min after the addition of G-CSF (Kanayasu-Toyoda et al., 2002) and that of p70 S6K was observed between 30 and 60 min after, indicating a lag time between PI3K and p70 S6K activation. It is conceivable that any signal molecule(s) must transduce the G-CSF signal during the time lag between PI3K and p70 S6K. Chung et al. (1994) also showed a lag time between PI3K and p70 S6K activation on HepG2 cells stimulated by platelet-derived growth factor (PDGF), suggesting that some signaling molecules also may transduce between PI3K and p70S6K.

Protein kinase C (PKC) is a family of Ser/Thr kinases involved in the signal transduction pathways that are triggered by numerous extracellular and intracellular stimuli. The PKC family has been shown to play an essential role in cellular functions, including mitogenic signaling, cytoskeleton rearrangement, glucose metabolism, differentiation, and the regulation of cell survival and apoptosis. Eleven different members of the PKC family have been identified so far. Based on their structural similarities and cofactor requirements, they have been grouped into three subfamilies: (1) the classical or conventional PKCs (cPKCα, β_1, β_2, and γ), activated by Ca^{2+}, diacylglycerol, and phosphatidyl-serine; (2) the novel PKCs (nPKCδ, ε, η, and θ), which are independent of Ca^{2+} but still responsive to diacylglycerol; and (3) the atypical PKCs (aPKCζ and ι/λ), where PKCλ is the homologue of human PKCι. Atypical PKCs differ significantly from all other PKC family

Abbreviations: DMSO, dimethyl sulfoxide; fMLP-R, formyl-Met-Leu-Phe receptor; RA, retinoic acid; G-CSF, granulocyte colony-stimulating factor; Trf-R, transferrin receptor; BSA, bovine serum albumin; FITC, fluorescein isothiocyanate; PBS, phosphate-buffered saline; PKC, protein kinase C; PI3K, phosphatidylinositol 3-kinase; p70 S6K, protein 70 S6 kinase; SDS–PAGE, sodium dodecyl sulfate-polyacrylamide gel electrophoresis; siRNA, small interfering RNA; PMN, polymorphonuclear leukocyte.

Contract grant sponsor: Ministry of Health, Labor, and Welfare of Japan.
Contract grant sponsor: Ministry of Education, Culture, Sports, Science, and Technology of Japan.

*Correspondence to: Teruhide Yamaguchi, Division of Cellular and Gene Therapy Products, National Institute of Health Sciences, 1-18-1, Kamiyoga, Setagaya-ku, Tokyo 158-8501, Japan.
E-mail: yamaguch@nihs.go.jp

Received 31 May 2006; Accepted 22 September 2006

Published online in Wiley InterScience (www.interscience.wiley.com.), 28 November 2006.
DOI: 10.1002/jcp.20930

members in their regulatory domains, in that they lack both the calcium-binding domain and one of the two zinc finger motifs required for diacylglycerol binding (Liu and Heckman, 1998). Romanelli et al. (1999) reported that p70 S6K is regulated by PKCζ and participates in a PI3K-regulated signaling complex. On the other hand, Selbie et al. (1993) reported that the tissue distribution of PKCζ is different from that of PKCι/λ, and that PKCι/λ appears to be widely expressed. If the p70 S6K could be activated by aPKC, the regulation of p70 S6K activation would seem to depend on the tissue-specific expression of PKCι and/or PKCζ. In neutrophilic lineage cells, the question is which aPKC participates in the regulation of p70 S6K on G-CSF signaling.

In this study, we show that G-CSF activated PKCι, promoting its translocation from the nucleus to the cell surface membrane and subsequently to the cytosol in DMSO-treated HL-60 cells. We also show the translocation of PKCι using myeloperoxidase-positive neutrophilic lineage differentiated from cord blood, which is a rich source of immature myeloid cells (Fritsch et al., 1993; Rappold et al., 1997; Huang et al., 1999; Debili et al., 2001; Hao et al., 2001). We concluded that PKCι translocation and activation by G-CSF are needed for neutrophilic proliferation.

Materials and Methods

Reagents

Anti-p70 S6K polyclonal antibody was obtained from Santa Cruz Biotechnology (Santa Cruz, CA). Anti-PKCι polyclonal antibody and monoclonal antibody were purchased from Santa Cruz Biotechnology and from Transduction Laboratories (Lexington, KY), respectively. Anti-PKCζ polyclonal antibody was purchased from Cell Signaling Technology (Beverly, MA). Anti-myeloperoxidase antibody was purchased from Serotec Ltd. (Oxford, UK). GF 109203X, and Gö 6983 were obtained from Calbiochem-Novabiochem (San Diego, CA). Wortmannin was obtained from Sigma Chemical (St. Louis, MO). Anti-Histon-H1 antibody, anti-Fcγ receptor IIa (CD32) antibody, and anti-lactate dehydrogenase antibody were from Upstate Cell Signaling Solutions (Lake Placid, NY), Lab Vision Corp. (Fremont, CA), and Chemicon International, Inc. (Temecula, CA), respectively.

Cell culture

HL-60, Jurkut, K562, U937, and THP-1 cells were kindly supplied by the Japanese Collection of Research Bioresources Cell Bank (Osaka, Japan). Cells were maintained in RPMI 1640 medium containing 10% heat-inactivated FBS and 30 mg/L kanamycin sulfate at 37°C in moisturized air containing 5% CO_2. The HL-60 cells, which were at a density of 2.5×10^5 cells/ml, were differentiated by 1.25% DMSO. Two days after the addition of DMSO, the G-CSF-induced signal transduction was analyzed using either magnetically sorted cells or non-sorted cells.

Magnetic cell sorting

To prepare Trf-R^- and Trf-R^+ cells, magnetic cell sorting was performed as previously reported (Kanayasu-Toyoda et al., 2002), using an automatic cell sorter (AUTO MACS; Miltenyi Biotec, Bergisch Gladbach, Germany). After cell sorting, both cell types were used for Western blotting and PKCι enzyme activity analyses.

Preparation of cell lysates and immunoblotting

For analysis of PKCι and PKCζ expression, a PVDF membrane blotted with 50 μg of various tissues per lane was purchased from BioChain Institute (Hayward, CA). Both a polymorphonuclear leukocytes (PMNs) fraction and a fraction containing lymphocytes and monocytes were isolated by centrifugation (400g, 25 min) using a Mono-poly resolving medium (Dai-Nippon Pharmaceutical, Osaka, Japan) from human whole blood, which was obtained from a healthy volunteer with informed consent. T-lymphocytes were further isolated from the mixture fraction using the Pan T Cell Isolation Kit (Miltenyi Biotec) according to the manufacturer's protocol. T-lymphocytes, PMNs, HL-60 cells, Jurkut cells, K562 cells, and U937 cells (1×10^7) were collected and lysed in lysis buffer containing 1% Triton X-100, 10 mM K_2HPO_4/KH_2PO_4 (pH 7.5), 1 mM EDTA, 5 mM EGTA, 10 mM $MgCl_2$, and 50 mM β-glycerophosphate, along with 1/100 (v/v protease inhibitor cocktail (Sigma Chemical) and 1/100 (v/v) phosphatase inhibitor cocktail (Sigma Chemical). The cellular lysate of 10^6 cells per lane was subjected to Western blotting analysis. Human cord blood was kindly supplied from the Metro Tokyo Red Cross Cord Blood Bank (Tokyo, Japan) with informed consent. Mononuclear cells isolated with the Lymphoprep™ Tube (Axis-Shield PoC AS, Oslo, Norway), were cultured in RPMI 1640 medium containing 10% FBS in the presence of G-CSF for 3 days. Cultured cells were collected, and the cell lysate was subjected to Western blotting analysis.

A fraction of the plasma membrane, cytosol, and nucleus of the DMSO-treated HL-60 cells was prepared by differential centrifugation after the addition of G-CSF, as described previously (Yamaguchi et al. 1999). After the cells that had been suspended in 250 mM sucrose/ 10 mM Tris-HCl (pH 7.4) containing 1/100 (v/v) protease inhibitor cocktail (Sigma Chemical) were gently disrupted by freezing and thawing, they were centrifuged at 800g, 4°C for 10 min. The precipitation was suspended in 10 mM Tris-HCl (pH 6.7) supplemented with 1% SDS. It was then digested by benzon nuclease at 4°C for 1 h and used as a sample of the nuclear fraction. After the post-nucleus supernatant was re-centrifuged at 100,000 rpm (452,000g) at a temperature of 4°C for 40 min, the precipitate was used as a crude membrane fraction and the supernatant as a cytosol fraction. Western blotting analysis was then performed as described previously (Kanayasu-Toyoda et al., 2002). The bands that appeared on x-ray films were scanned, and the density of each band was quantitated by Scion Image (Scion, Frederick, MD) using the data from three separate experiments.

Kinase assay

The activity of PKCι was determined by phosphorous incorporation into the fluorescence-labeled pseudosubstrate (Pierce Biotechnology, Rockford, IL). The cell lysates were prepared as described above and immunoprecipitated with the anti-PKCι antibody. Kinase activity was measured according to the manufacturer's protocol. In the analysis of inhibitors effects, cells were pretreated with a PI3K inhibitor, wortmannin (100 nM), or PKC inhibitors, GF109207X (10 μM) and Gö6983 (10 μM) for 30 min, and then stimulated by G-CSF for 15 min.

Observation of confocal laser-scanning microscopy

Upon the addition of G-CSF, PKCι localization in the DMSO-treated HL-60 cells for 2 days was examined by confocal laser-activated microscopy (LSM 510, Carl Zeiss, Oberkochen, Germany). The cells were treated with 50 ng/ml G-CSF for the indicated periods and then fixed with an equal volume of 4.0% paraformaldehyde in PBS(−). After treatment with ethanol, the fixed cells were labeled with anti-PKCι antibody and with secondary antibody conjugated with horseradish peroxidase. They were then visualized with TSA™ Fluorescence Systems (PerkinElmer, Boston, MA).

Mononuclear cells prepared from cord blood cells were cultured in RPMI 1640 medium containing 10% FBS in the presence of G-CSF for 7 days. Then, for serum and G-CSF starvation, cells were cultured in RPMI 1640 medium containing 1% BSA for 11 h. After stimulation by 50 ng/ml G-CSF, the cells were fixed, stained with both anti-PKCι polyclonal antibody and anti-myeloperoxidase monoclonal antibody, and finally visualized with rhodamine-conjugated anti-rabbit IgG and FITC-conjugated anti-mouse IgG, respectively.

RNA interference

Two pairs of siRNAs were chemically synthesized: annealed (Dharmacon RNA Technologies, Lafayette, CO) and transfected into HL-60 cells using Nucleofector™ (Amaxa, Cologne, Germany). The sequences of sense siRNAs were as follows: PKCι, GAAGAAGCCUUUAGACUUUTA; p70 S6K, GCAAGGAGUCUAUCCAUGAUU. As a control, the sequence ACUCUAUCGCCAGCGUGACUU was used. Forty-eight hours after treatment with siRNA, the cells were lysed for Western blot analysis. For proliferation and differentiation assay, cells were transfected with siRNA on the first day, treated with DMSO on the second day, and supplemented with G-CSF on the third day. After cells were subsequently cultured for 5 days, cell numbers and formyl-Met-Leu-Phe receptor (fMLP-R) expression were determined.

fMLP-R expression

The differentiated cells were collected and incubated with FITC-conjugated fMLP; then, labeled cells were subjected to flow cytometric analysis (FACSCalibur, Becton Dickinson, Franklin Lakes, NJ).

Statistical analysis

Statistical analysis was performed using unpaired Student's *t*-test. Values of $P < 0.05$ were considered to indicate statistical significance. Each experiment was repeated at least three times and representative data were indicated.

Results

The distribution of atypical PKC in various tissues and cells

Previously, we reported that the PI3K-p70 S6K-cMyc pathway plays an important role in the G-CSF-induced proliferation of DMSO-treated HL-60 cells, not only by enhancing the activity of both PI3K and p70 S6K but also by inducing the c-Myc protein (Kanayasu-Toyoda et al., 2002, 2003). We also reported that G-CSF did not stimulate Erk1, Erk2, or 4E-binding protein 1. The maximum kinase activity of PI3K was observed 5 min after the addition of G-CSF, and that of p70 S6K was observed between 30 and 60 min after. It is conceivable that any signal molecule(s) must transduce the G-CSF signal during the time lag between PI3K and p70 S6K. Romanelli et al. (1999) suggested that the activation of p70 S6K is regulated by PKCξ and participates in the PI3K-regulated signaling complex. To examine the role of atypical PKC in the G-CSF-dependent activation and the relationship between atypical PKC and p70 S6K, the protein expression of PKCζ and PKCι in various human tissues and cells was analyzed by Western blotting. As shown in Figure 1A, both of the atypical PKCs were markedly expressed in lung and kidney but were weakly expressed in spleen, stomach, and placenta. In brain, cervix, and uterus, the expression of only PKCι was observed. Selbie et al. (1993) have reported observing the expression of PKCζ not in protein levels but in RNA levels, in the kidney, brain, lung, and testis, and that of PKCι in the kidney, brain, and lung. In this study, the protein expression of PKCι in the kidney, brain, and lung was consistent with the RNA expression of PKCι. Despite the strong expression of PKCζ RNA in brain (Selbie et al., 1993), PKCζ protein was scarcely observed. Although PKCι proteins were scarcely expressed in neutrophils and T-lymphocytes in peripheral blood, they were abundantly expressed in immature blood cell lines, that is, Jurkut, K562, U937, and HL-60 cells (Fig. 1B), in contrast with the very low expression of PKCζ proteins. In mononuclear cells isolated from umbilical cord blood, which contains large numbers of immature myeloid cells and has a high proliferation ability, the expression of PKCι proteins was also observed. Since Nguyen and Dessauer (2005) have reported observing abundant PKCζ proteins in THP-1 cells, as a positive control for PKCζ, we also performed a Western blot of THP-1 cells (Fig. 1B, right part). While PKCι was markedly expressed in both THP-1 and HL-60 cells, PKCζ was observed only in THP-1 cells.

These data suggested that PKCζ and PKCι were distributed differently in various tissues and cells, and that mainly PKCι proteins were expressed in proliferating blood cells.

Stimulation of PKCι activity by G-CSF

Among the 11 different members of the PKC family, the aPKCs (ζ and ι/λ) have been reported to activate p70 S6K activity and to be regulated by PI3K (Akimoto et al., 1998; Romanelli et al., 1999). As shown in Figure 1, although the PKCζ proteins were not detected by Western blotting in HL-60 cells or mononuclear cells isolated from cord blood cells, it is possible that PKCι could functionally regulate p70 S6K as an upstream regulator in these cells. Therefore, we focused on the role of PKCι as the possible upstream regulator of p70 S6K in neutrophil lineage cells. First, we compared the expression of PKCι in both Trf-R^+ and Trf-R^- cells. PKCι proteins were expressed more abundantly in Trf-R^+ cells than in Trf-R^- cells (Fig. 2A, middle part), as with the p70 S6K proteins. A time course study of PKCι activity upon the addition of G-CSF revealed the maximum stimulation at 15 min, lasting until 30 min. The G-CSF-dependent activation of PKCι was inhibited by the PKC inhibitors wortmannin, GF 109203X, and Gö 6983. Considering the marked inhibitory effect of wortmannin on PKCι and evidence that the maximum stimulation of PI3K was observed at 5 min after the addition of G-CSF, PI3K was determined to be the upstream regulator of PKCι in the G-CSF signal transduction of HL-60 cells. The basal activity of PKCι in Trf-R^+ cells was higher than that in Trf-R^- cells, and G-CSF was more augmented. In Trf-R^- cells, PKCι activity was scarcely stimulated by G-CSF. This tendency of PKCι to be activated by G-CSF was similar to that of PI3K (Kanayasu-Toyoda et al., 2002).

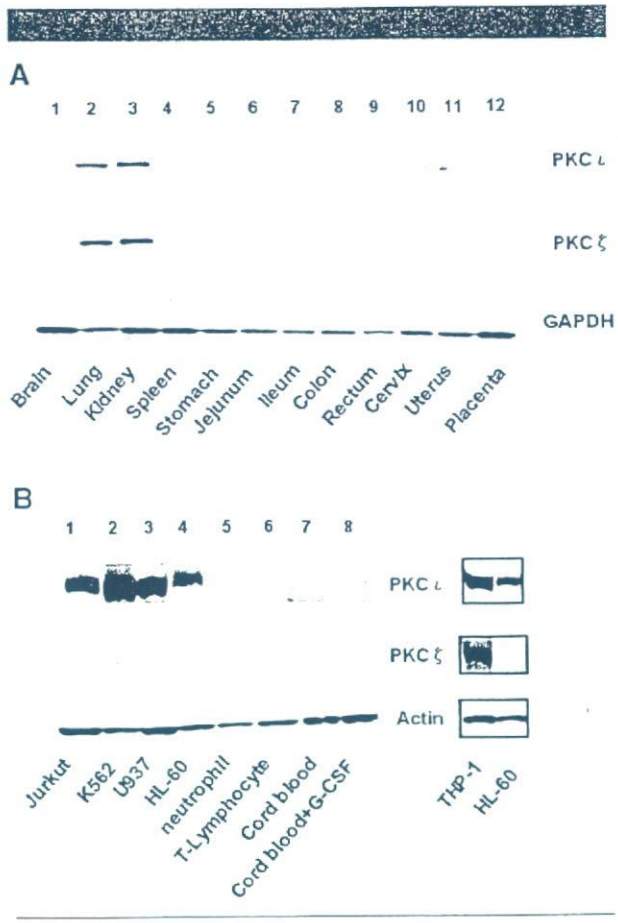

Fig. 1. Different distributions of PKCζ and PKCι. The protein expression of PKCι appears in the upper part and that of PKCζ in the middle part in various tissues and cells. A: 1, brain; 2, lung; 3, kidney, 4, spleen; 5, stomach; 6, jejunum; 7, ileum; 8, colon; 9, rectum; 10, cervix; 11, uterus; 12, placenta. Anti-GAPDH blot is a control for various tissues. B: 1, jurkut cells; 2, K562 cells; 3, U937 cells; 4, HL-60 cells; 5, neutrophils; 6, T-lymphocytes; 7, mononuclear cells from cord blood in the absence of G-CSF; 8, mononuclear cells from cord blood in the presence of G-CSF. Anti-actin blot is a control. The right part shows immunoblots of PKCι, PKCζ, and actin of THP-1 cells as a positive control for PKCζ. The cell numbers of THP-1 and HL-60 cells were adjusted in relation to other cells on the left parts.

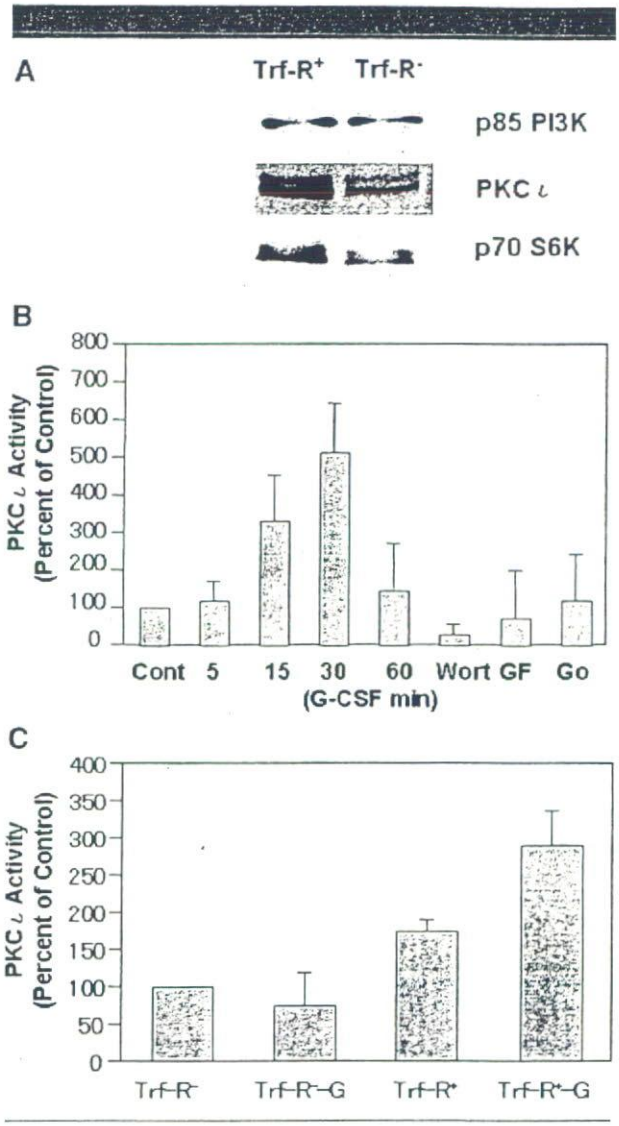

Fig. 2. Expression of PKCι in Trf-R$^+$ and Trf-R$^-$ cells and effects of G-CSF on PKCι activity. A: The expression of PKCι in Trf-R$^+$ and Trf-R$^-$ cells was subjected to Western blot analysis after magnetic cell sorting. B: The G-CSF-dependent PKCι activation of the DMSO-treated HL-60 cells was measured. The x-axis represents the time lapse (min) after the G-CSF stimulation and the y-axis percent of control that was not stimulated by G-CSF. Columns and bars represent the mean ± SD, using data from three separate experiments. Wort: wortmannin (100 nM), GF: GF109207X (10 μM), Gö: Gö6983 (10 μM). Cells were pretreated with each inhibitor and then stimulated by G-CSF for 15 min. C: The PKCι activity in the Trf-R$^+$ and Trf-R$^-$ cells 30 min after the addition of G-CSF. The y-axis represents the percentage of control that was non-stimulated Trf-R$^-$ cells. Columns and bars represent the mean ± SD, using data from three separate experiments.

Effects of G-CSF on PKCι translocation

Muscella et al. (2003) demonstrated that the translocation of PKCζ from the cytosol to the nucleus or membrane is required for c-Fos synthesis induced by angiotensin II in MCF-7 cells. It was also reported that high glucose induced the translocation of PKCι (Chuang et al., 2003). These results suggest that the translocation of aPKC plays an important role in its signaling. To clarify the translocation of PKCι, immuno-histochemical staining (Fig. 3) and biochemical fractionation (Fig. 4) in DMSO-induced HL-60 cells were performed after the addition of G-CSF. In a non-stimulated condition, PKCι in the HL-60 cells treated with DMSO for 2 days (Fig. 3, control) was detected mainly in the nucleus. Analysis of Western blotting (Fig. 4, left parts) and quantification of the bands (Fig. 4, right columns) also revealed that PKCι was localized and observed mainly in the nuclear fraction (Fig. 4A). During the 5–15 min period after the addition of G-CSF, PKCι was found to translocate (Figs. 3 and 4B) into the membrane fraction, after which it re-translocated into the cytosol fraction (Fig. 4C). In the presence of wortmannin, the G-CSF-induced translocation of PKCι into the plasma membrane failed, but PKCι was found to localize in the cytosolic fraction (Figs. 3 and 4B). Myeloperoxidase is thought to be expressed in stage from promyelocytes to mature neutrophils (Manz et al., 2002). In human cord blood cells (Fig. 3), PKCι in the cells co-stained with anti-myeloperoxidase antibody was also localized in the nucleus after serum depletion (Fig. 3B top parts). Ten minutes after the addition of G-CSF, PKCι was found to translocate into the membrane, and then into the cytosol at 30 min after the addition of G-CSF. In the presence of wortmannin, the G-CSF-induced translocation of PKCι into the plasma membrane failed but PKCι was found to localize in the cytosol. This suggested that the dynamic translocation of PKCι induced by G-CSF is a universal phenomenon in neutrophilic lineage cells. Taken together, these data support the possibility that PI3K plays not only an important role upstream of PKCι but also triggers the translocation from nucleus to membrane upon the addition of G-CSF.

In order to assess the purity of each cellular fraction, antibodies against specific markers were blotted. As specific markers, Histon-H1, Fcγ receptor IIa (CD32), and lactate dehydrogenase (LDH) were used for the nuclear, membrane, and cytosolic fractions, respectively. The purities of the nuclear, membrane, and cytosolic fractions were 82.0, 78.5, and 72.2%, respectively (Fig. 4D).

Effects of siRNA for PKCι on proliferation and differentiation

To determine the role of PKCι in neutrophilic proliferation and differentiation, PKCι was knocked down by siRNA. When the protein level of PKCι was specifically downregulated by siRNA for PKCι (Fig. 5A), G-CSF failed to enhance proliferation of the cells during 5 days' cultivation (Fig. 5B). The effect of siRNA for PKCι on neutrophilic differentiation in terms of fMLP-R expression was also determined. As shown in Figure 5C, fMLP-R expression was promoted by siRNA for PKCι in either the presence (lower part) or absence (upper part) of G-CSF. These data indicate that PKCι positively regulates G-CSF-induced proliferation and negatively regulates the differentiation of DMSO-treated HL-60 cells.

Discussion

We previously reported that PI3K/p70 S6K plays an important role in the regulation of the neutrophilic differentiation and proliferation of HL-60 cells. Akimoto et al. (1998) and Romanelli et al. (1999) reported that p70 S6K is regulated by aPKC and aPKCλ/PKCζ, respectively. At first, we showed that the distribution of PKCζ and PKCι proteins in various human tissues and cells was not similar (Fig. 1A), and that PKCι are more abundantly expressed in proliferating blood cells: Jurkut, K562, U937, and HL-60 cells (Fig. 1B). Moreover, PKCι proteins were also observed in cultured mononuclear cells of cord blood, in which the myeloid progenitors were enriched in the presence or absence of G-CSF (Fig. 1B). The myeloperoxidase-positive cells as neutrophilic lineage cells, a myeloid marker, were also stained with the antibody of PKCι (Fig. 3B). Although PKCζ proteins are barely detected in

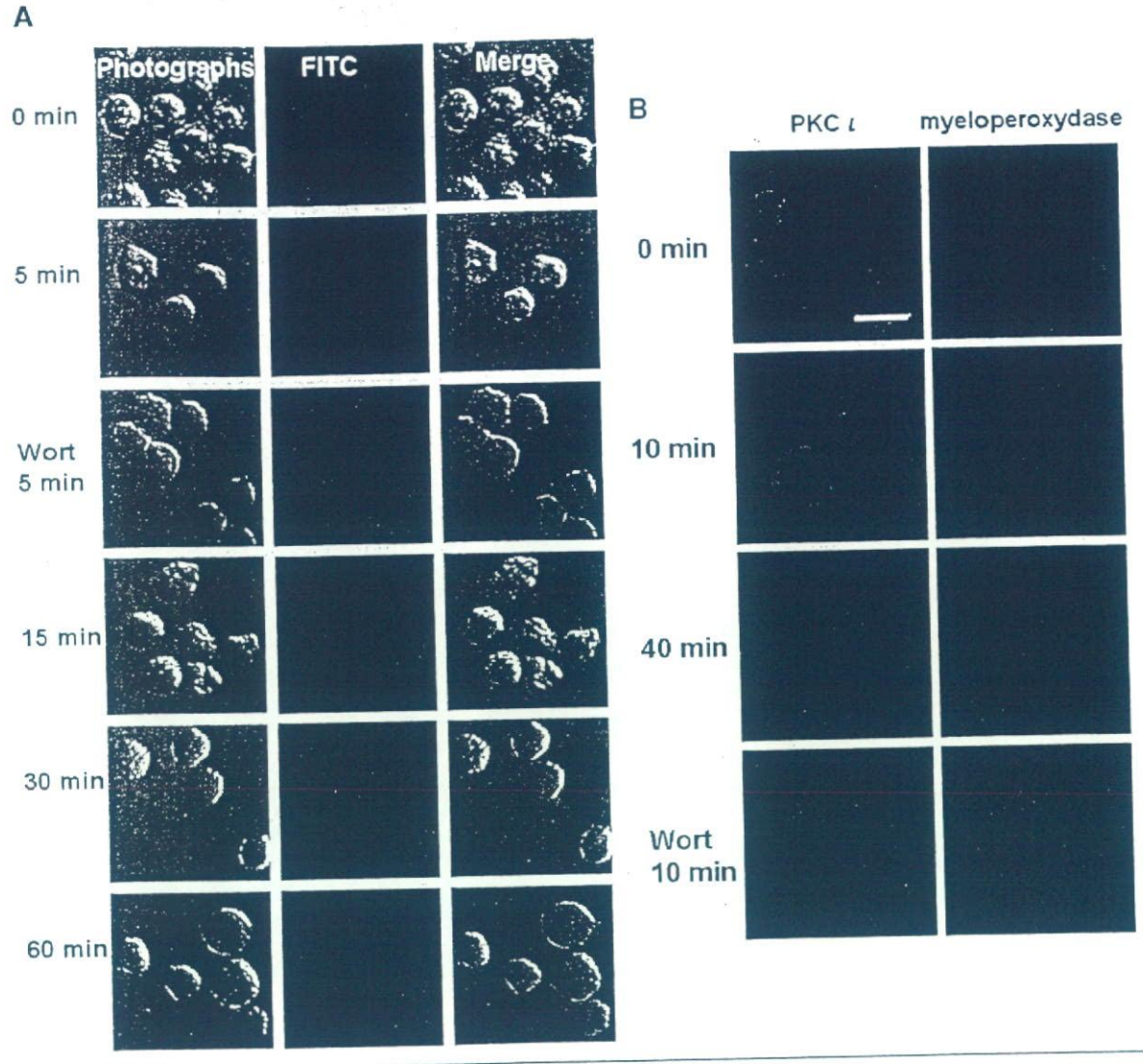

Fig. 3. Translocation of PKCι after the activation of G-CSF. A: 2 days after the addition of DMSO, HL-60 cells stimulated by G-CSF were fixed, incubated with anti-PKCι antibody, and visualized as described above. The photographs can be seen at the left part of the figure, the fluorescent photographs in the middle of the figure, and the merged images at the right. B: G-CSF-stimulated mononuclear cells from cord blood were stained with anti-PKCι antibody (red, left part) and anti-myeloperoxidase antibody (green, right part) after serum depletion. Under no stimulation, PKCι was observed in the nucleus. G-CSF promoted the translocation of PKCι to the membrane within 5–15 min, and then to the cytosol. Wort: wortmannin. White bar: 10 μm.

neutrophilic HL-60 cells, PKCι proteins were markedly expressed in these cells (Fig. 1B). This study showed, for the first time, the stimulation of PKCι activity in G-CSF-treated HL-60 cells (Fig. 2B) at 15–30 min after the addition of G-CSF. Maximum activation from the addition of NGF in PC12 cells was also observed at 15 min (Wooten et al., 2001).

Atypical PKCs are lipid-regulated kinases that need to be localized to the membrane in order to be activated. PKCζ is directly activated by phosphatidylinositol 3,4,5-trisphosphate, a product of PI3K (Nakanishi et al., 1993). We previously reported that the maximum activation of PI3K was observed in HL-60 cells 5 min after the addition of G-CSF (Kanayasu-Toyoda et al., 2002). Most investigators have reported the translocation of aPKC in either muscle cells or adipocytes stimulated by insulin (Andjelkovic et al., 1997; Goransson et al., 1998; Galetic et al., 1999; Standaert et al., 1999; Braiman et al., 2001; Chen et al., 2003; Kanzaki et al., 2004; Sasaoka et al., 2004; Herr et al., 2005). In response to insulin stimulation, aPKCζ/λ is translocated to the plasma membrane (Standaert et al., 1999; Braiman et al., 2001), where aPKCζ/λ is believed to be activated (Galetic et al., 1999; Kanzaki et al., 2004). In the present study, the addition of G-CSF induced PKCι to translocate to the membrane from the nucleus within 5–15 min (Figs. 3 and 4), and this translocation to the plasma membrane accompanied the full activation of PKCι (Fig. 2B). Previously we reported also that the maximum activation of p70 S6K in HL-60 cells was observed from 30 to 60 min after the addition of G-CSF (Kanayasu-Toyoda et al., 1999, 2002), suggesting that there was a time lag between the activation of PI3K and p70 S6K upon the addition of G-CSF in HL-60 cells. In the present study, PKCι was

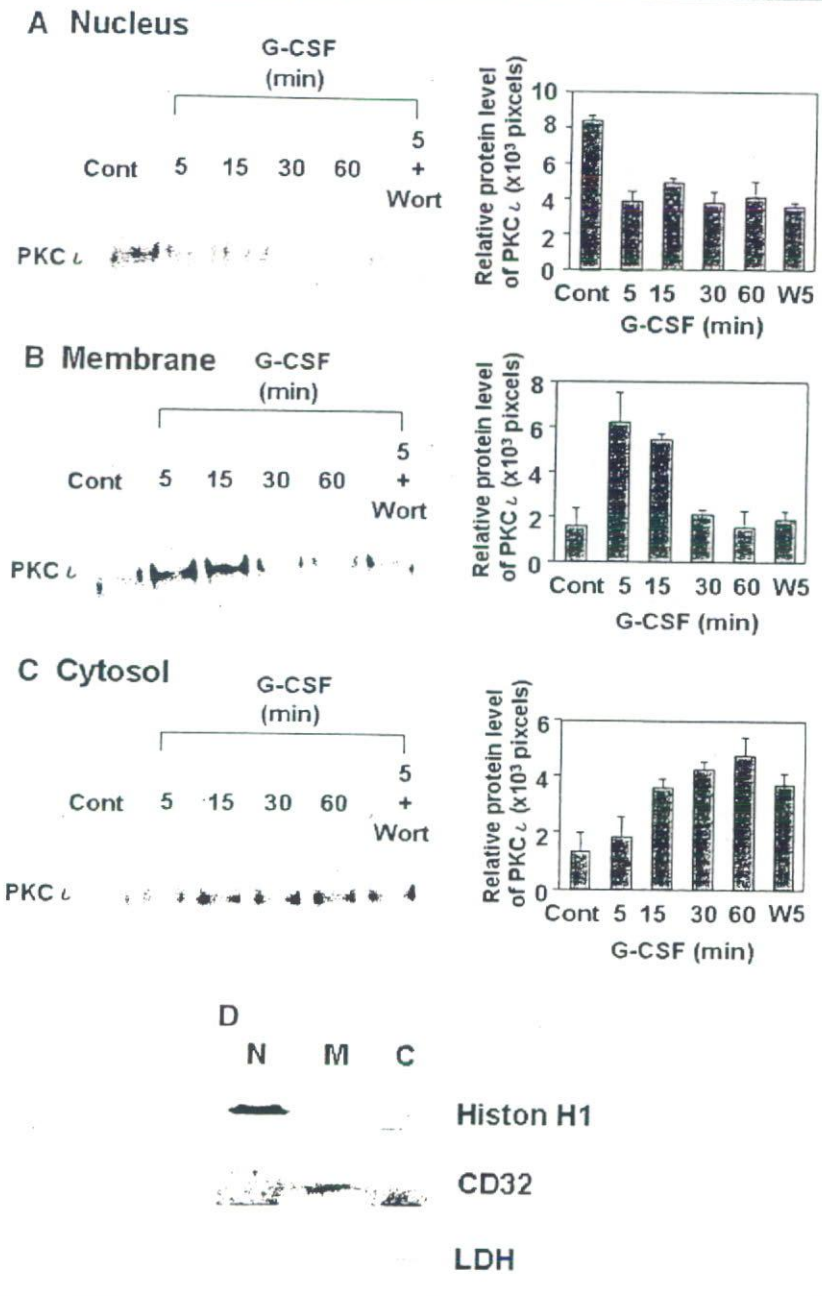

Fig. 4. Translocation of PKCι after activation by G-CSF on biochemical fractionation. The cells were differentiated as described in the Figure 3 legend. After stimulation by G-CSF, the amounts of PKCι proteins in the nucleus (A), plasma membrane (B), and cytosol (C), as fractionated by differential centrifugation, were analyzed by Western blotting (left parts). The right parts show the quantitation of the bands of PKCι proteins. Wort or W: wortmannin. PKCι protein was quantitated using data from three separate experiments. Columns and bars represent the mean ± SD. D: Each cell fraction was immunoblotted with antibodies of specific marker. Histon-H1, Fcγ receptor IIa (CD32), and lactate dehydrogenase (LDH) are specific markers for nuclear (N), membrane (M), and cytosolic (C) fractions, respectively.

found to re-translocate from the plasma membrane to the cytosol (Figs. 3 and 4C). In the presence of wortmannin, an inhibitor of PI3K, PKCι failed to translocate into the plasma membrane, but instead translocated to cytosol directly from the nucleus upon the addition of G-CSF (Figs. 3 and 4B). PKCι translocation was also observed in myeloperoxidase-positive cells derived from human cord blood (Fig. 3B), indicating that G-CSF-induced dynamic translocation of PKCι occurred in not only a limited cell line but also neutrophilic lineage cells. These data suggest that PI3K plays an important role in the activation and translocation of PKCι during the G-CSF-induced activation of myeloid cells. Furthermore, the translocation to the plasma membrane in response to G-CSF is wortmannin sensitive, but the translocation from the nucleus upon G-CSF stimulation is not affected by wortmannin, suggesting that the initial signal of G-CSF-induced PKCι translocation from the nucleus may be

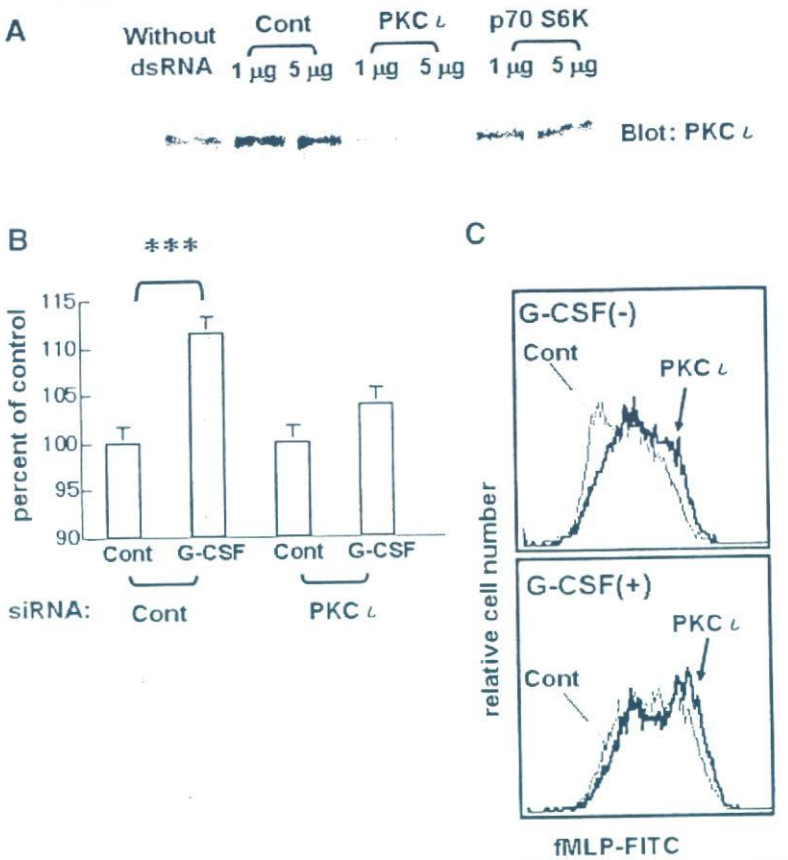

Fig. 5. Effects of siRNA of PKCι on proliferation, differentiation, and phosphorylation at various sites of p70 S6K. A: Forty-eight hours after transfection with siRNA of PKCι or p70 S6K, protein levels of PKCι were compared. B: Proliferation of the cells transfected with siRNA of PKCι or control (Cont) was measured 5 days after the addition of G-CSF. Columns and bars represent the mean ± SD of triplicate wells (***$P < 0.001$). C: fMLP-R expression was analyzed by flow cytometry 5 days after the addition of G-CSF. The gray arrow indicates cells transfected with the control sequence of double-stranded RNA (Cont, gray lines), and the black arrow the cells transfected with siRNA for PKCι (black lines) in the presence (lower part) or absence (upper part) of G-CSF.

PI3K-independent, but association of PKCι with the plasma membrane could be mediated through a PI3K-dependent signal. Cord blood is an important material of blood transplantation for leukemia (Bradstock et al., 2006; Ooi, 2006; Yamada et al., 2006) or for congenital neutropenia (Mino et al., 2004; Nakazawa et al., 2004) because it contains many hematopoietic stem cells such as CD34-positive cells or CD133-positive cells, and also contains immature granulocytes. The neutrophilic differentiation and proliferation are necessary processes after transplantation.

Formyl-Met-Leu-Phe peptide evokes the migration, superoxide production, and phagocytosis of neutrophils through fMLP-R, a suitable marker for neutrophilic differentiation. In this study, the reduction of PKCι by siRNA inhibited G-CSF-induced proliferation (Fig. 5B) and promoted neutrophilic differentiation (Fig. 5C) in terms of fMLP-R expression. These data, however, suggest that PKCι promoted G-CSF-induced proliferation and blocked differentiation at the same time.

The substrates of aPKC have recently been reported: namely, the cytoskeletal protein Lethal giant larvae (Lgl) was phosphorylated by Drosophila aPKC (Betschinger et al., 2003) and glyceraldehydes-3-phosphate dehydrogenase (GAPDH) was phosphorylated by PKCι (Tisdale, 2002) directly in both cases. While the direct phosphorylation of p70 S6K by aPKC was not observed (Akimoto et al., 1998; Romanelli et al., 1999), the enzyme activity of p70 S6K was markedly enhanced by co-transfection with aPKC and PDK-1, the latter of which is recruited to the membrane due to the binding of phosphatidylinositol-3,4,5-trisphosphate to its PH domain (Anderson et al., 1998). The addition of G-CSF induced PKCι to increase phosphorylation at Thr-389, which is the site most closely related to enzyme activity among the multi-phosphorylation sites of p70 S6K (Weng et al., 1998). However, the mammalian target of rapamycin (mTOR), an upstream regulator, also phosphorylates Thr-389 of p70 S6K and markedly stimulates p70 S6K activity under coexistence with PDK-1 (Isotani et al., 1999). We could not rule out the possibility that other PKC isoforms can contribute to the activation of p70 S6K. We postulated that in G-CSF-stimulated HL-60 cells, PKCι contributes to p70 S6K activation as an upstream regulator.

Atypical PKC isoforms are reported to play an important role in the activation of IκB kinase β (Lallena et al., 1999). In PKCζ-deficient mice, impaired signaling through the B-cell receptor resulted in the inhibition of cell proliferation and survival while also causing defects in the activation of ERK and the transcription of NF-κB-dependent genes (Martin et al., 2002). Moreover, Lafuente et al. (2003) demonstrated that the loss of Par-4, that is, the genetic inactivation of the aPKC inhibitor, led to an increased proliferative response of